

Review

How Much Potential Do Nucleoside Analogs Offer to Combat Human Corona Viruses?

Włodzimierz Buchowicz * and Mariola Koszytkowska-Stawińska * 

Faculty of Chemistry, Chair of Organic Chemistry, Warsaw University of Technology, Noakowskiego 3, 00-664 Warsaw, Poland

* Correspondence: wlodzimierz.buchowicz@pw.edu.pl (W.B.); mariola.koszytkowska@pw.edu.pl (M.K.-S.)

Abstract: Nucleoside analogs (NAs) have been extensively examined as plausible antiviral agents in recent years, in particular since the outbreak of the global pandemic of COVID-19 in 2019. In this review, the structures and antiviral properties of over 450 NAs are collected according to the type of virus, namely SARS-CoV, SARS-CoV-2, MERS-CoV, HCoV-OC43, HCoV-229E, and HCoV-NL63. The activity of the NAs against HCoV-related enzymes is also presented. Selected studies dealing with the mode of action of the NAs are discussed in detail. The repurposing of known NAs appears to be the most extensively investigated scientific approach towards efficacious anti-HCoV agents. The recently reported de novo-designed NAs seem to open up additional approaches to new drug candidates.

Keywords: coronavirus; drug development; nucleoside analogs; drug repurposing

1. Introduction

The family of human corona viruses (HCoVs) includes seven strains [1]. Four of them, namely HCoV-229E, HCoV-HKU1, HCoV-NL63, and HCoV-OC43, cause mild and self-limiting infections of the upper respiratory tract. However, two HCoVs are responsible for serious respiratory disease epidemics that originated in China in 2002 and 2003 (severe acute respiratory syndrome coronavirus, SARS-CoV virus) and in Saudi Arabia in 2012 (Middle East respiratory syndrome coronavirus, MERS-CoV virus) [2]. Starting in November 2002, followed by spreading to 29 countries, the SARS-CoV virus caused approximately 8000 illnesses and 700 deaths from late 2002 to late 2003 [3]. Then, it disappeared. The MERS-CoV virus is endemic to the Middle East [4]. However, due to travelers' migration, MERS-CoV virus infections have been reported in 27 countries, resulting in 858 known deaths since 2012 [5]. The SARS-CoV-2 virus (severe acute respiratory syndrome coronavirus 2) is responsible for the pandemic of coronavirus disease (COVID-19) that started in China in 2019. As of 28 May 2023, over 767 million confirmed cases of COVID-19 and over 6.9 million deaths have been reported globally [6]. The end of COVID-19 as a public health emergency was declared in May 2023 [7]. However, continuous mutations of the SARS-CoV-2 virus and the risk of its new variants emerging elsewhere have been emphasized.

Very close similarity has been found between SARS-CoV [8], MERS-CoV [9], and SARS-CoV-2 [10] in terms of their genome sequences and the key proteins involved in the virus life cycle and entry process. These findings have provided solid arguments for postulates on the possible susceptibility of SARS-CoV, MERS-CoV, and SARS-CoV-2 viruses to the same or structurally similar antiviral agents [11–13].

A significant number of approved antiviral or anticancer drugs belong to the class of nucleoside analogs (NAs). Many of them show multitarget activity [14]. For this reason, considerable attention has been paid to NAs as potential anticoronavirus drug candidates since the SARS-CoV outbreak in 2002. Initial efforts to treat SARS-CoV-infected patients focused on the use of ribavirin due to its activity against a broad spectrum of RNA or DNA viruses, including RSV, influenza viruses, and parainfluenza viruses [15]. Further studies



Citation: Buchowicz, W.; Koszytkowska-Stawińska, M. How Much Potential Do Nucleoside Analogs Offer to Combat Human Corona Viruses? *Organics* **2024**, *5*, 71–110. <https://doi.org/10.3390/org5020006>

Academic Editor: Wim Dehaen

Received: 27 September 2023

Revised: 1 April 2024

Accepted: 11 April 2024

Published: 8 May 2024



Copyright: © 2024 by the authors. Licensee MDPI, Basel, Switzerland. This article is an open access article distributed under the terms and conditions of the Creative Commons Attribution (CC BY) license (<https://creativecommons.org/licenses/by/4.0/>).

suggested the limited usefulness of ribavirin in the treatment of SARS-CoV patients [16]. A few NAs with promising activity against SARS-CoV-2 viruses were identified before or during the SARS-CoV-2 pandemic. Among them, remdesivir, molnupiravir, and VV116 have been approved for the treatment of COVID-19 in selected countries (Figure 1) [17].

Very recently, the FDA granted fast-track designation for the investigational drug bemnifosbuvir (Figure 1), which is in a global phase III clinical trial SUNRISE-3 (NCT05629962) for outpatients with high risk of disease progression [18].

The selected NAs as potential anti-HCoV agents have been discussed in several review articles within the last five years. These reviews have mainly mentioned either remdesivir or a very narrow group of NAs [19–25]. Particular emphasis has been on compounds with known mechanisms of action against SARS-CoV-2 (Figure 1) [26–28]. Although the susceptibility of HCoVs to a variety of NAs has been studied for over twenty years, only a few original publications have been included in a review discussing a relatively broad group of twenty-four NAs with micromolar activity against SARS-CoV, SARS-CoV-2 or MERS-CoV, and HCoV-NL63 [29]. The activity of NAs against HCoVs other than SARS-CoV, SARS-CoV-2, or MERS-CoV has been mentioned infrequently [20,25,29].

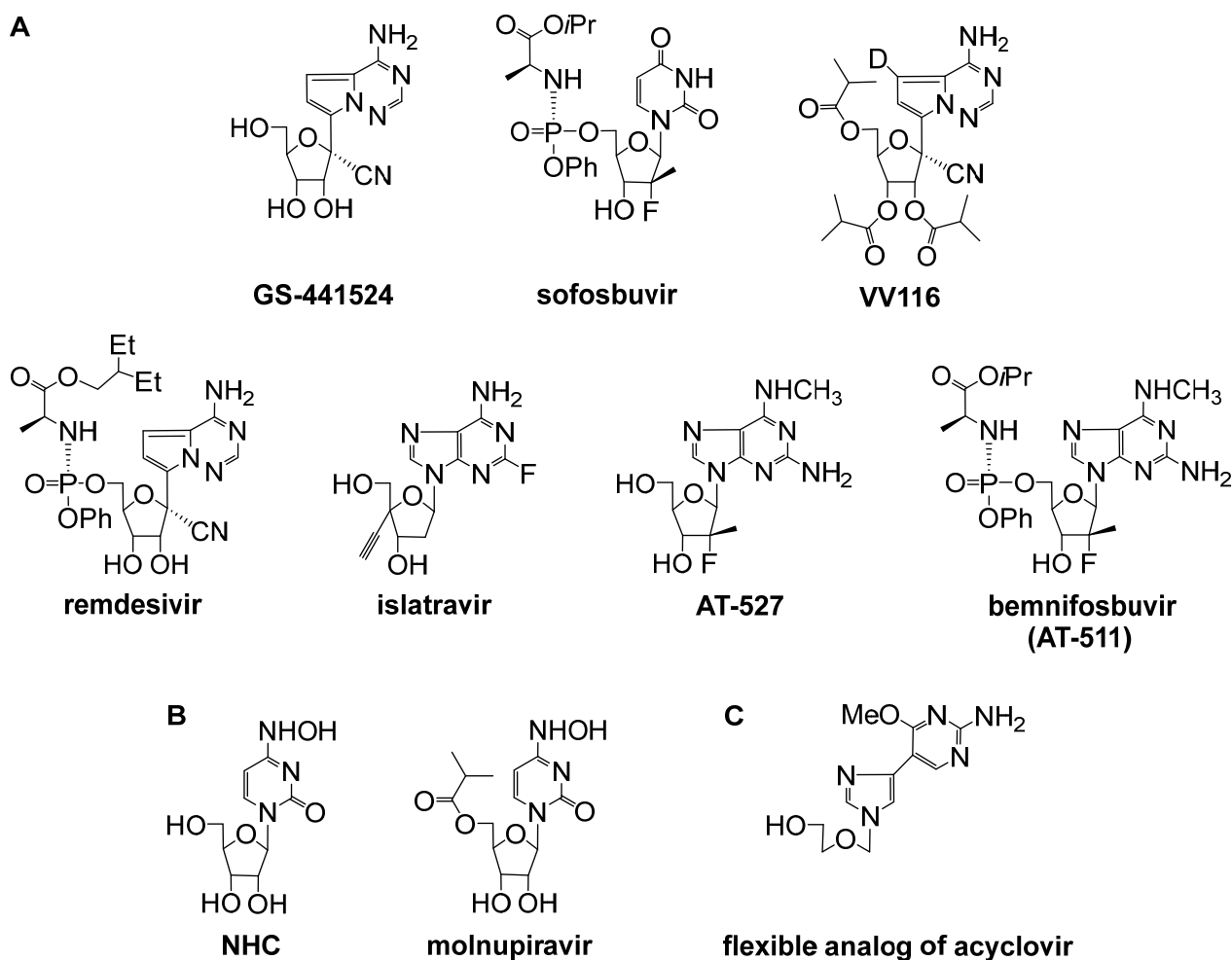


Figure 1. NAs with well-recognized activity and modes of action against HCoVs. (A) RNA chain terminators, including those acting with a dual mechanism of action (remdesivir, islatravir, AT-527, and bemnifosbuvir) [26]. (B) NAs causing lethal mutagenesis. (C) NAs inhibiting viral methyltransferases.

The aim of our review is to discuss a very broad panel of NAs reported to show *in vitro* inhibition of the replication of a specific HCoV. We collected over 450 compounds from 80 original works published from 2003 to August 2023. Our intention is to illustrate the

importance of NAs (both those existing in the public domain and those newly designed) in the state-of-the-art development of anti-HCoV agents. Therefore, we also included NAs displaying moderate or low activity. All the presented compounds are summarized in Tables 1–6. The NAs reported to inhibit HCoV-related enzyme(s) are collected in Table 7. In order to show research trends in the development of nucleoside anti-HCoV agents, we divided the discussed NAs into four groups. That is, depending on the reported drug research and development (DRD) approach, the NAs are arranged as those found from the following: the repurposing of known NAs, including approved drugs or their prodrugs (approach A); the development of prodrugs of known anti-HCoV NAs (approach B); structural modifications of anti-HCoV NAs, leading to their nonprodrug analogs (approach C); or the development of de novo-designed NAs (approach D). Within each defined approach A, B, C, or D, the NAs are ordered in Tables 1–7 according to the year of publication. Within a pool of NAs depicted with a general structure, we show the antiviral activity of the most active compound, or the one demonstrating the highest SI. When applicable, International Nonproprietary Names (INNs) or abbreviations of NAs are given in order to facilitate their identification. The abovementioned NAs with well-recognized activity and their mode of action against HCoVs (Figure 1) are included in this review in order to maintain the clarity of the collected data. Owing to the fact that some of these compounds have been often employed as reference compounds in antiviral assays, only their effective concentration values reported in the original publications are cited. The goal of this review is to discuss NAs with anti-HCoV activity in the context of their chemical structure and diversity. The results of studies dealing with the mode of action of the examined compounds are presented in detail.

1.1. The Nucleoside Analogs Evaluated as In Vitro Inhibitors of SARS-CoV Replication

The NAs examined in vitro for their inhibitory activity against SARS-CoV are shown in Table 1. Two DRD approaches were employed in order to find effective agents against SARS-CoV: the repurposing of existing NAs (approach A) and the development of de novo-designed NAs (approach D). Besides NHC (entry 1.11), ribavirin (entry 1.12), remdesivir (entry 1.31), and compounds AT-511 (entry 1.32) and GS-441524 (entry 1.37), the approved nucleoside drugs (zalcitabine, entry 1.3; cidofovir, entry 1.5; mizoribine, entry 1.13; gemcitabine, entry 1.28; or acyclovir, entry 1.30) and their analogs (acyclovir analogs, entry 1.7; tenofovir analogs, entry 1.8; adefovir analogs, entry 1.10; mizoribine analog, entry 1.14; AZT analogs, entries 1.17 and 1.16; clofarabine analog, entry 1.24; and analogs of remdesivir parent nucleoside GS-441524, entry 1.36) represent a relatively large group of the examined compounds. DNA canonical nucleosides (2'-deoxycytidine, entry 1.3 and 2'-deoxyadenosine, entry 1.6) or natural noncanonical nucleosides (pyrazofurin, entry 1.2, and neplanocin A, entry 1.25) were also studied. The other repurposed NAs (approach A) were derived from typical structural modifications, such as (a) the acylation/alkylation of the functional groups in the parent nucleoside (entry 1.3), (b) the incorporation of additional substituent(s) (e.g., an alkyl group or a halogen atom) into the scaffold of the parent nucleoside (entry 1.3), (c) the replacement of the nucleobase nitrogen by a carbon atom (entries 1.4 and 1.6), (d) the replacement of the parent nucleobase or sugar with its synthetic surrogate (entries 1.9, 1.20, 1.22, and 1.27), (e) the “dehydration” of the sugar moiety (entry 1.18), and/or (f) the conjugation of an artificial glycone and an artificial nucleobase (entry 1.29). L-nucleoside analogs have also been reported (entries 1.15, 1.19, 1.21, 1.23, 1.26, and 1.29). However, comparative evaluations of the enantiomeric NAs are infrequent (entries 1.18 vs. 1.19, 1.20 vs. 1.21, and 1.25 vs. 1.26). The de novo-designed NAs (approach D) were developed through (a) the conjugation of a glycone and a nucleobase derived from different parent nucleosides (entry 1.33; ribavirin and neplanocin A, respectively) and the subsequent preparation of the nucleobase-modified analogs; (b) the conjugation of an artificial nucleobase with a furanose (entry 1.35, chloropurine) or the glycone derived from a drug (penciclovir) or its cyclobutyl analog (entry 1.34); or (c) the fluorination of the parent nucleoside (aristeromycin) followed by the preparation of the nucleobase-modified analogs or prodrugs (entry 1.38).

The majority of the NAs evaluated as anti-SARS-CoV agents featured two-digit micromolar activity (for compounds with one-digit micromolar or submicromolar activity, see entries 1.2, 1.3, 1.6, 1.11, 1.13, 1.31, 1.32, 1.37, and 1.38). Among the NAs endowed with submicromolar activity, only fluorinated analogs of aristeromycin (entry 1.38) belong to the group of de novo-designed NAs.

Table 1. The nucleoside analogs evaluated in vitro against the replication of SARS-CoV.

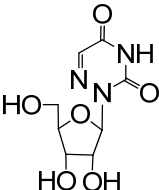
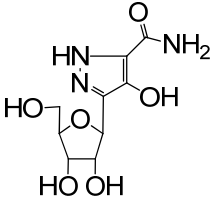
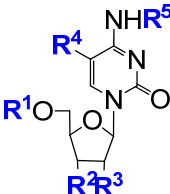
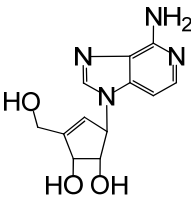
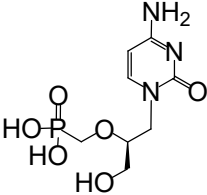
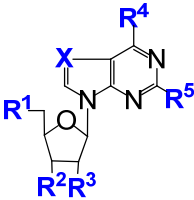
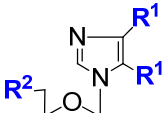
Entry ^a /DRD Approach, Structure, and Number of Compounds Examined	Effective Concentration Value ^b ; Cell Line; Virus Variant (If Given) Cytotoxic Concentration Value ^c ; Cell Line Selectivity Index ^d (SI, If Given)	Ref.	
1.1/A 	6-azauridine EC ₅₀ 16.8 (2.9) mg/L; Vero; FFM-1 (FFM-2) CC ₅₀ 104 (18) mg/L; Vero SI 6	[30]	
1.2/A 	pyrazofurin EC ₅₀ 4.2 (0.57) mg/L; Vero; FFM-1 (FFM-2) CC ₅₀ 52 (9.6) mg/L; Vero SI 12	[30]	
1.3/A 	R ¹ = H or DMTr R ² = H or OH R ³ = H, OH, OMe R ⁴ = H, Me, Br, Cl R ⁵ = H, Bz, Ac (10 compounds)	R ¹ , R ² , R ⁴ , R ⁵ = H, R ³ = OMe: EC ₅₀ 4 μM; Vero 76; Urbani IC ₅₀ 23 μM; Vero 76 SI 6	[31]
1.4/A 	3-deazaneplanocin A	EC ₅₀ > 380 μM; Vero E6; Urbani IC ₅₀ > 380 μM; Vero E6	[31]
1.5/A 	cidofovir	EC ₅₀ > 360 μM; Vero 76; Urbani IC ₅₀ > 360 μM; Vero 76	[31]
1.6/A 	R ¹ , R ² , R ³ = H or OH R ⁴ = OH or NH ₂ R ⁵ = H or NH ₂	2'-deoxytubercidin (R ¹ , R ² = OH, R ³ , R ⁵ = H, R ⁴ = NH ₂ , X = CH): EC ₅₀ 0.1 μM; Vero E6; Urbani IC ₅₀ 0.4 μM; Vero E6 SI 4	[31]
1.7/A 	R ¹ = CN, CO ₂ H R ² = OH, OAc, OBn, Br, P(O)(OEt) ₂ (5 compounds)	R ¹ = CN, R ² = OAc: IC ₅₀ 15 μg/mL; Vero CC ₅₀ 56 μg/mL; Vero	[33]

Table 1. Cont.

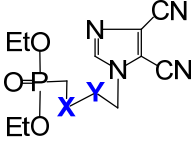
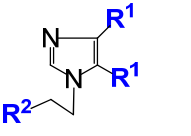
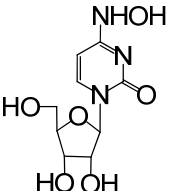
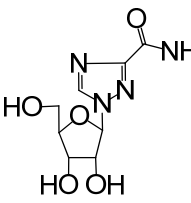
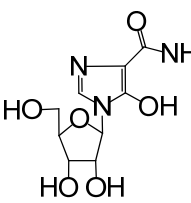
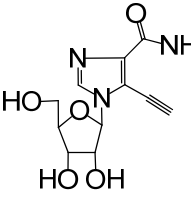
Entry ^a /DRD Approach, Structure, and Number of Compounds Examined	Effective Concentration Value ^b ; Cell Line; Virus Variant (If Given) Cytotoxic Concentration Value ^c ; Cell Line Selectivity Index ^d (SI, If Given)	Ref.	
1.8/A 	X, Y = CH ₂ or O (2 compounds)	X = CH ₂ , Y = O: IC ₅₀ 23 µg/mL; Vero CC ₅₀ > 75 µg/mL; Vero	[33]
1.9/A 	R ¹ = Tol, H, Bz, Ac R ² = H, OH, OAc, OBz, R ³ = CN, CO ₂ Me, C(O)NHNH ₂ , C(O)NH ₂ (7 compounds)	R ¹ , R ² = H, R ³ = CO ₂ Me: IC ₅₀ 18 µg/mL; Vero CC ₅₀ > 75 µg/mL; Vero	[33]
1.10/A 	R ¹ = CN, CO ₂ H CO ₂ Me, R ² = OH, OAc, P(O)(OH) ₂ (4 compounds)	R ¹ = CO ₂ Me, R ² = OH: IC ₅₀ 28 µg/mL; Vero CC ₅₀ > 75 µg/mL; Vero	[33]
1.11/A 	NHC	EC ₅₀ 5 µM; Vero E6; Urbani IC ₅₀ 50 µM; Vero E6 SI 10	[31]
1.12/A 	ribavirin	IC ₅₀ 0.1 ± 0.0 µM; Vero; Urbani CC ₅₀ 12.5 ± 3.5 µM; Vero 76 SI > 125	[32]
		IC ₅₀ from 50 to 100 µg/mL; fRhK4; ten clinical isolates CC ₅₀ > 1000 µg/mL; fRhK4 SI from 50 to >80	[34]
		IC ₅₀ 20 ± 15 µg/mL; Vero E6; Frankfurt-1 CC ₅₀ 40 µg/mL; Vero E6 (2 virus variants evaluated)	[35]
		IC ₅₀ 210 µM; Vero 76; Urbani CC ₅₀ 283 µM; Vero 76 SI 1	[16]
1.13/A 	mizoribine	IC ₅₀ 0.14 µM; HAE; GFP	[36]
		IC ₅₀ 3.5 ± 2.9 µg/mL; Vero E6; Frankfurt-1 CC ₅₀ > 200 µg/mL; Vero E6 (2 virus variants)	[35]
1.14/A 	EICAR	IC ₅₀ > 40 µM; Vero 76; Urbani CC ₅₀ > 40 µM; Vero 76 SI 0 ^e	[16]
		IC ₅₀ 13.5 µM; Vero E6; Frankfurt-1 CC ₅₀ > 700 µM; Vero E6 SI > 52	[37]

Table 1. Cont.

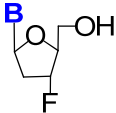
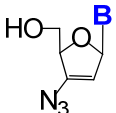
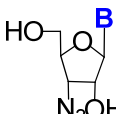
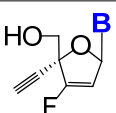
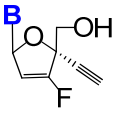
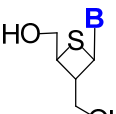
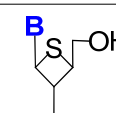
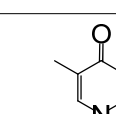
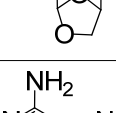
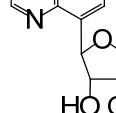
Entry ^a /DRD Approach, Structure, and Number of Compounds Examined	Effective Concentration Value ^b ; Cell Line; Virus Variant (If Given) Cytotoxic Concentration Value ^c ; Cell Line Selectivity Index ^d (SI, If Given)	Ref.	
1.15/A 	B = 5-chlorouracil-1-yl, thymine-1-yl, cytosine-1-yl, uracil-1-yl, adenine-1-yl	B = 5-chlorouracil-1-yl: EC ₅₀ < 10 μM; Vero 76 IC ₅₀ 28 μM; Vero 76 SI > 2.8	[38]
1.16/A 	B = thymine-1-yl, cytosine-1-yl, adenine-1-yl or guanine-1-yl	B = thymine-1-yl: EC ₅₀ 10.3 μM; Vero 76 IC ₅₀ 16.1 μM; Vero 76 SI 1.6	[38]
1.17/A 	B = thymine-1-yl, adenine-1-yl or guanine-1-yl	B = adenine-1-yl: EC ₅₀ 11.1 μM; Vero 76 IC ₅₀ 3.5 μM; Vero 76 SI 0 ^e	[38]
1.18/A 	B = cytosine-1-yl, adenine-1-yl or thymine-1-yl	B = adenine-1-yl: EC ₅₀ 11.1 μM; Vero 76 IC ₅₀ 14.5 μM; Vero 76 SI 1.3	[38]
1.19/A 	B = adenine-1-yl, thymine-1-yl or cytosine-1-yl	B = adenine-1-yl: EC ₅₀ 11.9 μM; Vero 76 IC ₅₀ 25.6 μM; Vero 76 SI 2.2	[38]
1.20/A 	B = thymine-1-yl, uracil-1-yl, adenine-1-yl, inosine-1-yl or guanine-1-yl	B = thymine-1-yl: EC ₅₀ 20 μM; Vero 76 IC ₅₀ > 100 μM; Vero 76 SI 5	[38]
1.21/A 	B = uracil-1-yl, cytosine-1-yl, adenine-1-yl, inosine-1-yl or guanine-1-yl	B = cytosine-1-yl: EC ₅₀ 20 μM; Vero 76 IC ₅₀ 20 μM; Vero 76 SI 1	[38]
1.22/A 	dioxolane T (DOT)	EC ₅₀ 24.5 μM; Vero 76 IC ₅₀ > 100 μM; Vero 76 SI 4.1	[38]
1.23/A 	HCl	EC ₅₀ 28.6 μM; Vero 76 IC ₅₀ > 18.8 μM; Vero 76 SI 0	[38]
1.24/A 		EC ₅₀ 76.8 μM; Vero 76 IC ₅₀ > 100 μM; Vero 76 SI 1.3	[38]

Table 1. Cont.

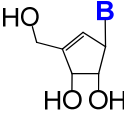
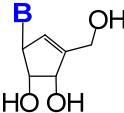
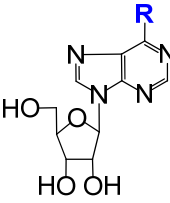
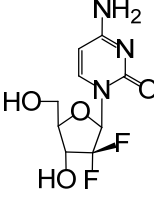
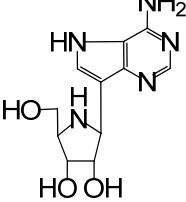
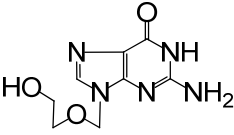
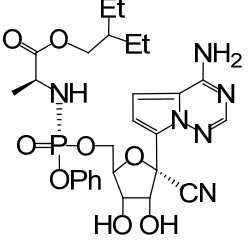
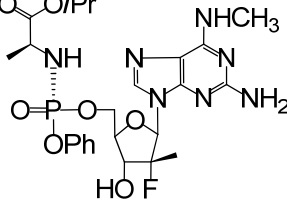
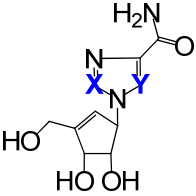
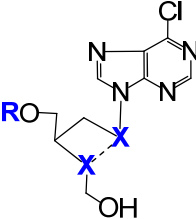
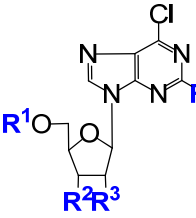
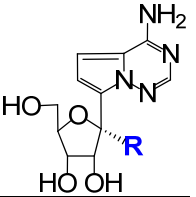
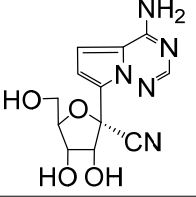
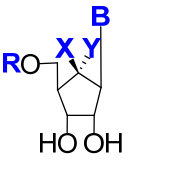
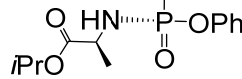
Entry ^a /DRD Approach, Structure, and Number of Compounds Examined	Effective Concentration Value ^b ; Cell Line; Virus Variant (If Given) Cytotoxic Concentration Value ^c ; Cell Line Selectivity Index ^d (SI, If Given)	Ref.	
1.25/A 	B = thymine-1-yl, N-OH-cytosine-1-yl, adenine-1-yl (neplanocin A) or inosine-1-yl	EC ₅₀ > 100 μM; Vero 76 IC ₅₀ > 10 μM; Vero 76 SI 0	[38]
1.26/A 	B = thymine-1-yl or inosine-1-yl	EC ₅₀ > 100 μM; Vero 76 IC ₅₀ > 100 μM; Vero 76 SI 0	[38]
1.27/A 	R = OMe or SMe	IC ₅₀ > 300 μM; Vero E6; Frankfurt-1	[37]
1.28/A 	gemcitabine	EC ₅₀ 4.957 μM; Vero E6	[39]
1.29/A ^e 	galidesivir (BCX4430, immucillin-A)	EC ₅₀ 57.7 μM; Urbani CC ₅₀ > 296 μM; Vero 76 SI > 5.1	[40]
1.30/A 	acyclovir	EC ₅₀ > 1000 μM; Vero E6; Frankfurt-1 CC ₅₀ > 1000 μM; Vero E6	[41]
1.31/A 	remdesivir	IC ₅₀ 0.069 ± 0.036 μM CC ₅₀ > 10 μM; HAE SI > 100	[42,43]
1.32/A 	AT-511 (bemnifosbuvir, free form of AT-527)	EC ₉₀ 0.34 μM CC ₅₀ > 86 μM; Huh7 SI > 250	[44]

Table 1. Cont.

Entry ^a /DRD Approach, Structure, and Number of Compounds Examined	Effective Concentration Value ^b ; Cell Line; Virus Variant (If Given) Cytotoxic Concentration Value ^c ; Cell Line Selectivity Index ^d (SI, If Given)	Ref.		
1.33/D		X, Y = CH or N(3 compounds)	X = CH, Y = N: EC ₅₀ 21 μM IC ₅₀ > 100 μM SI > 4.8	[45]
1.34/D		R = H or Bz X---X = CH-CH or X = CH ₂ (4 compounds)	R = Bz, X---X = CH-CH: IC ₅₀ 14.5 μM; Frankfurt-1 CC ₅₀ 78 μM; Vero E6 SI 5.4	[37]
1.35/D		R ¹ = H or Bz R ² , R ³ = H or OH R ⁴ = H or NH ₂ (5 compounds)	R ¹ , R ² , R ³ = OH, R ⁴ = H: IC ₅₀ 48.7 μM; Vero E6; Frankfurt-1 CC ₅₀ 279 μM; Vero E6 SI 5.7	[37]
1.36/D		R = Me, vinyl, ethynyl	R = vinyl: EC ₅₀ 14.0 μM; Vero; Toronto-2 CC ₅₀ > 30 μM; Vero	[46]
1.37/D		GS-441524	IC ₅₀ 0.18 ± 0.14 μM; HAE CC ₅₀ > 100 μM; HAE	[42,43]
1.38/D ^e		X, Y = H or F B = uracil-1-yl, cytosin-1-yl N ⁶ -Me-adenin-1-yl, adenin-1-yl, R = H or	X, Y = F, B = adenin-1-yl, R = H: EC ₅₀ 0.5 μM; Vero E6; Frankfurt 1 CC ₅₀ 5.9 μM; Vero E6 SI 11.8	[47]
 (12 compounds)				

Approach A: repurposing of the known NAs, including approved drugs or their prodrugs. Approach D: development of de novo-designed NAs. ^a Entry numbers include the number of the table and the position of a compound (or a group of compounds) on the timeline, taking into account the year of publication of the references discussed. ^b Exemplified as the effective compound concentration (EC₅₀ or EC₉₀ or IC₅₀). ^c Exemplified as the cytotoxic compound concentration (CC₅₀ or IC₅₀). ^d Defined as the ratio of the compound cytotoxic concentration and the compound effective concentration. Only values explicitly given by the authors are cited. Values SI 0 are given according to the authors. ^e See text for details.

Galidesivir was reported by Bavari and coworkers to be active against a wide range of ssRNA(+) and ssRNA(−) viruses, with its inhibitory effect against SARS-CoV (entry 1.29, EC₅₀ 57.7 μM, CC₅₀ > 296 μM) and MERS-CoV (entry 3.2, EC₅₀ 68.4 μM, CC₅₀ > 100 μM) [40]. Galidesivir's mechanism of action was postulated to involve its rapid phosphorylation to galidesivir–triphosphate, followed by the pyrophosphate cleavage and incorporation of galidesivir–monophosphate into nascent viral RNA strands. Experiments with HCV RNA polymerase supported this hypothesis and showed that galidesivir targeted the RNA-dependent RNA polymerase (RdRp) of RNA viruses. It also inhibited the polymerase function by inducing nonobligate RNA chain termination. It was suggested that the termination occurred two bases after the incorporation of galidesivir–monophosphate. An incorporation of galidesivir–monophosphate into human RNA or DNA was not observed. A clinical trial of galidesivir for the treatment of yellow fever or COVID-19 was initiated in April 2020 in Brazil [48]. The results from the trial in COVID-19 patients showed that galidesivir was safe and well tolerated. The therapy was associated with a dose-dependent decline in viral levels of SARS-CoV-2 in the respiratory tract. However, no clinical efficacy benefit with galidesivir treatment compared to a placebo treatment was observed in the trial. Thus, a discontinuation of the pursuit of a COVID-19 indication for galidesivir was announced [49]. The potential of galidesivir against SARS-CoV-2 has been further explored (entry 2.13), including efficacy studies in an animal model [50].

Besides the 1'-branched NAs (entry 1.36) designed upon the development of the remdesivir parent nucleoside GS-441524 (entry 1.37), the NAs designed de novo in search for anti-SARS-CoV agents (approach D) include the following: the azole analogs of neplanocin A (entry 1.33), cyclic or acyclic 6-chloropurine analogs (entries 1.34 and 1.35), and the 6'-fluoro derivatives of (−)-aristeromycin (entry 1.38). Among the 6'-fluoro analogs of (−)-aristeromycin (entry 1.38), the 6',6'-difluoro analog (X,Y = F; B = adenin-1-yl) displays submicromolar activity against the selected +RNA viruses, including SARS-CoV (entry 1.38, EC₅₀ 0.5 μM) and MERS-CoV (entry 3.10, EC₅₀ 0.2 μM) [47]. Structure–activity relationship (SAR) studies showed that an adenin-1-yl ring and two fluorine atoms were required for anti-SARS-CoV activity. However, Calu-3-based assays revealed a significant decrease in the activity of this compound, not only towards MERS-CoV but also towards SARS-CoV and SARS-CoV-2. Interestingly, the phosphoramidate prodrug of the most active compound (X,Y = F; B = adenin-1-yl) was less antivirally active (SARS-CoV, EC₅₀ 6.8 μM) and more toxic towards the host *Vero E6* cells. The antiviral activity of this compound was postulated to be due to an (indirect) effect on the viral MTase activity through the inhibition of host SAH hydrolase. Preliminary assays also identified the in vitro activity of this compound against SARS-CoV-2 (entry 2.39, EC₅₀ ~2 μM). Regardless of the cell line, the monophosphoramidate prodrug of the 6',6'-difluoro analog (X,Y = F; B = adenin-1-yl) was also less active against MERS-CoV (EC₅₀ 9.3 μM) than its parent compound [51]. The 6',6'-difluoro analog (X,Y = F; B = adenin-1-yl) demonstrated inhibition at an early stage of MERS-CoV replication. However, the development of MERS-CoV mutants strongly resistant to this compound was observed.

1.2. The Nucleoside Analogs Evaluated as In Vitro Inhibitors of SARS-CoV-2 Replication

The NAs examined in vitro for their inhibitory activity against SARS-CoV-2 are collected in Table 2. Considering that SARS-CoV-2 emerged just a short time ago, the known NAs (approach A, entries 2.1–2.30) are the broadest group of the assayed compounds. Among them, compounds endowed with submicromolar activity belong to the following groups: (a) approved drugs (gemcitabine, entry 1.19; or forodesine, entry 1.26); (b) natural non-canonical nucleosides (tubercidin and its derivatives, entries 2.10, 2.13–2.16, and 2.31; sangivamycin, entry 2.22; or riboprine, entry 2.25); and (c) drug metabolites (thioguanosine, entry 2.18) or their analogs (entry 2.20). Studies on the novel prodrugs of GS-441524 or NHC (approach B, entries 2.32–2.35) have been reported since 2021. These prodrugs were the 5'-O-phosphoric/carboxylic esters of GS-441524 (entries 2.34 and 2.33, respectively) or the 4-O-carboxylic/carboxylic esters of NHC (entry 2.35). Among them, compounds with submicromolar activity were found. The structural modifications of the anti-HCoV NAs

leading to their nonprodrug analogs (approach C) involved the fluorination or deuteration of the nucleobase in GS-441524 (entry 2.36 and 2.37, respectively) or the fluorination of the sugar moiety in NHC (entry 2.38). Among these modifications, the deuteration of GS-441524 was the most successful. The isobutyric triester of the 7-deutero derivative showed submicromolar activity (entry 2.37). Very few de novo-designed NAs (approach D) are represented by the 6',6'-difluoro derivatives of (–)-aristeromycin (entry 2.39) and the 2'-branched analogs of the selected canonical nucleosides (entry 2.40). These compounds showed moderate inhibitory activity against SARS-CoV-2 in vitro, albeit accompanied by considerable cytotoxicity.

Table 2. The nucleoside analogs evaluated in vitro against the replication of SARS-CoV-2.

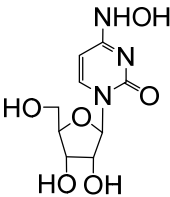
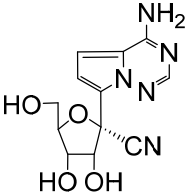
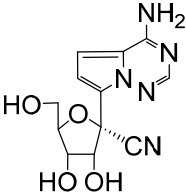
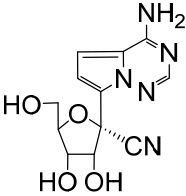
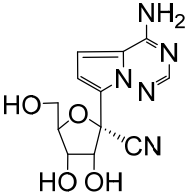
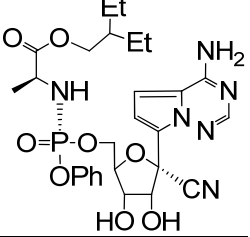
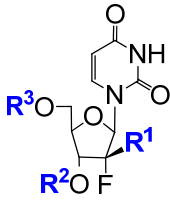
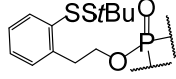
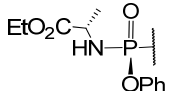
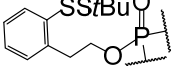
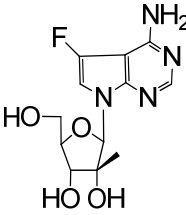
Entry ^a /DRD Approach, Structure and Number of Compounds Examined	Effective Concentration Value ^b ; Cell Line; Virus Variant (If Given) Cytotoxic Concentration Value ^c ; Cell Line Selectivity Index ^d (SI, If Given)	Ref.	
2.1/A 	NHC IC ₅₀ 0.08 μM; Calu-3	[36]	
2.2/A 	GS-441524 EC ₅₀ 0.3 ± 0.2 μM; Vero CC ₅₀ 12.6 μM; Vero SI 42	[52]	
2.2/A 	GS-441524 EC ₅₀ 8.2 ± 0.4 μM; Vero CC ₅₀ > 100 μM; Vero SI 12	[52]	
2.2/A 	GS-441524 EC ₅₀ 0.59 ± 0.10 μM; Vero E6 CC ₅₀ > 500 μM; Vero E6 SI > 847.46 (2 virus variants evaluated)	[53]	
2.2/A 	GS-441524 EC ₅₀ 0.10 μM; Calu-3; WA1 CC ₅₀ > 50 μM; Calu-3 SI > 524	[54]	
2.3/A 	remdesivir EC ₅₀ 1.0 ± 0.1 μM; Vero CC ₅₀ > 100 μM; Vero SI > 100	[52]	
2.4/A 	R ¹ = Me, Cl, Br R ² , R ³ =  or R ² = H and  R ³ = (4 compounds)	R ¹ = Me, R ² , R ³ =  EC ₅₀ 6.3 ± 0.1 μM; Vero CC ₅₀ 16.4 μM; Vero	[52]
2.5/A 	EC ₅₀ 7.6 ± 0.4 μM; Vero CC ₅₀ > 100 μM; Vero SI > 10	[52]	

Table 2. Cont.

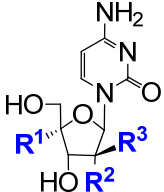
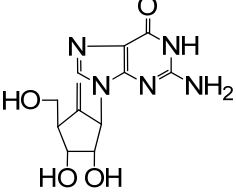
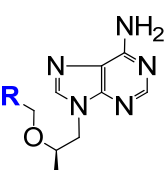
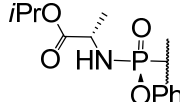
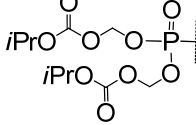
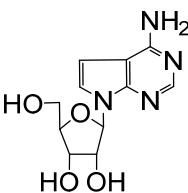
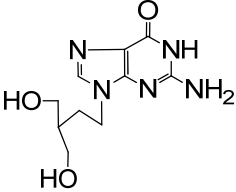
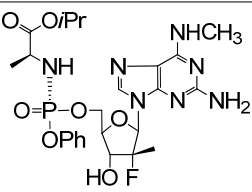
Entry ^a /DRD Approach, Structure and Number of Compounds Examined	Effective Concentration Value ^b ; Cell Line; Virus Variant (If Given) Cytotoxic Concentration Value ^c ; Cell Line Selectivity Index ^d (SI, If Given)	Ref.	
2.6/A	 <p>2'-MeC: R¹ = H, R² = OH, R³ = Me ALS-8112: R¹ = CH₂Cl, R² = F, R³ = H</p>	<p>2'-MeC: EC₅₀ 9.2 ± 0.1 μM; <i>Vero</i> CC₅₀ > 100 μM; <i>Vero</i> SI > 10</p>	[52]
2.7/A	 <p>entecavir</p>	<p>EC₅₀ > 20 μM; <i>Vero</i> CC₅₀ > 20 μM; <i>Vero</i></p>	[52]
2.8/A	 <p>lamivudine: R = H emtricitabine: R = F</p>	<p>lamivudine and emtricitabine EC₅₀ > 20 μM; <i>Vero</i> CC₅₀ > 20 μM; <i>Vero</i></p>	[52]
2.9/A	 <p>tenofovir alafenamide:  R = tenofovir isoproxil:  R =</p>	<p>tenofovir alafenamide and tenofovir isoproxil: EC₅₀ > 20 μM; <i>Vero</i> CC₅₀ > 20 μM; <i>Vero</i></p>	[52]
2.10/A ^d	 <p>tubercidin</p>	<p>EC₅₀ 0.77 μM; <i>Vero E6</i> CC₅₀ > 100 μM; <i>Vero E6</i> SI 129.87</p>	[55]
2.11/A	 <p>penciclovir</p>	<p>EC₅₀ 95.96 μM; <i>Vero E6</i> CC₅₀ > 400 μM; <i>Vero E6</i> SI 4.17</p>	[55]
2.12/A	 <p>AT-511 (bemnifosbuvir, free form of AT-527)</p>	<p>EC₉₀ 0.47 ± 0.12 μM; <i>HAE</i> CC₅₀ > 86 μM; <i>HAE</i> SI > 160</p>	[44]

Table 2. Cont.

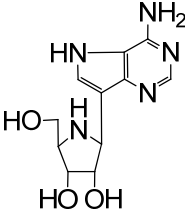
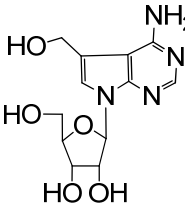
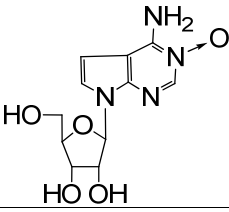
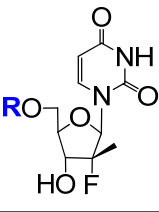
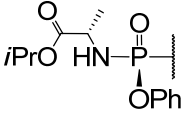
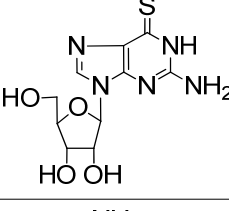
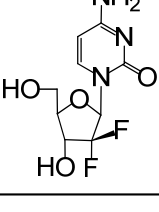
Entry ^a /DRD Approach, Structure and Number of Compounds Examined	Effective Concentration Value ^b ; Cell Line; Virus Variant (If Given) Cytotoxic Concentration Value ^c ; Cell Line Selectivity Index ^d (SI, If Given)	Ref.		
2.13/A ^e		galidesivir (BCX4430, immucillin-A)	EC ₅₀ 14.15 μM; <i>Calu-3</i> ; WA1/2020 CC ₅₀ > 50 μM; <i>Calu-3</i> SI > 3.5	[50]
2.14/A ^e		5-hydroxymethyltubercidin	EC ₉₀ 0.57 μM; <i>Caco-2</i> ; WK-521 CC ₅₀ > 50 μM; <i>MRC5</i>	[56]
2.15/A ^e		R ¹ = H or CN R ² = H, CH=NOH, NO ₂ Me, CN (5 compounds)	R ¹ = H, R ² = CH=NOH: EC ₉₀ 0.20 μM; <i>Caco-2</i> ; WK-521 CC ₅₀ 0.74 μM; <i>MRC5</i>	[56]
2.16/A ^e			EC ₉₀ 3.5 μM <i>Caco-2</i> ; WK-521 CC ₅₀ 24 μM; <i>MRC5</i>	[56]
2.17/A		R = H or 	Sofosbuvir, R = EC ₅₀ 5.1 ± 0.8 μM, <i>Huh-7</i> ; clinic isolate CC ₅₀ 381 ± 34 μM, <i>Huh-7</i> SI 74	[57]
2.18/A		thioguanosine	EC ₅₀ 0.04 μM; <i>Calu-3</i> ; WA1 CC ₅₀ 1.14 μM; <i>Calu-3</i> SI 26	[54]
2.19/A		gemcitabine	EC ₅₀ 0.04 μM; <i>Calu-3</i> ; WA1 CC ₅₀ > 20 μM; <i>Calu-3</i> SI > 1235	[54]

Table 2. Cont.

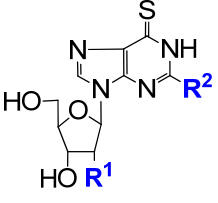
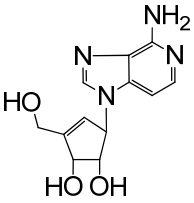
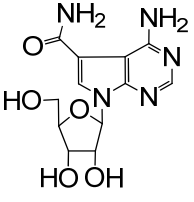
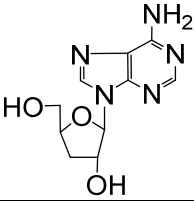
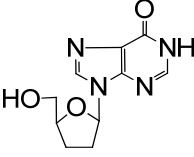
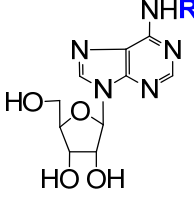
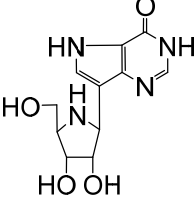
Entry ^a /DRD Approach, Structure and Number of Compounds Examined	Effective Concentration Value ^b ; Cell Line; Virus Variant (If Given) Cytotoxic Concentration Value ^c ; Cell Line Selectivity Index ^d (SI, If Given)	Ref.	
2.20/A 	R ¹ = H or OH R ² = H or NH ₂ (2 compounds)	6-thioinosine (R ¹ = OH, R ² = H): EC ₅₀ 0.05 μM; Calu-3; WA1 CC ₅₀ > 50 μM; Calu-3 SI > 1083	[54]
2.21/A 	3-deazaneplanocin A	IC ₅₀ 579 nM; SARS-CoV-2; A549-nRFP-ACE2; SARS-CoV-2-MUC-IMB-1 (in combination with remdesivir)	[59]
2.22/A ^e 	sangivamycin	EC ₅₀ 15.4 nM; Vero E6; B.1.1.7 (Alpha) SI 39.0 (8 virus variants evaluated)	[60]
2.23/A ^e 	cordycepin	EC ₅₀ 2.01 ± 0.12 μM; Vero E6; VOC-202012/01 CC ₅₀ > 100 μM; Vero E6	[61]
2.24/A ^e 	didanosine	EC ₅₀ 3.10 ± μM; Vero E6; VOC-2020/01 CC ₅₀ > 100 μM; Vero E6	[62]
2.25/A ^e 	riboprime: R = 3-methylbut-2-en-1-yl tecadenoson: R = (R)-tetrahydrofuran-3-yl	riboprime: EC ₅₀ 408 ± 22 nM; Vero E6; Omicron B.1.1.529/BA.5; CC ₅₀ > 100 μM; Vero E6 (3 virus variants evaluated)	[63–66]
2.26/A ^e 	forodesine	EC ₅₀ 657 ± 34 nM; Vero E6; Omicron B.1.1.529/BA.5 CC ₅₀ > 100 μM; Vero E6 (3 virus variants evaluated)	[63–66]

Table 2. Cont.

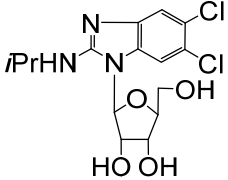
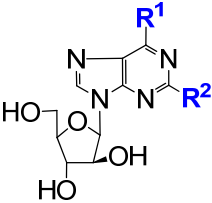
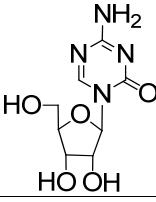
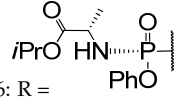
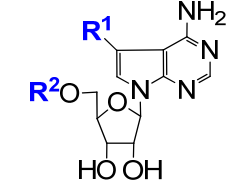
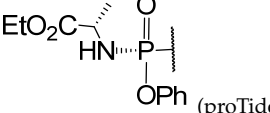
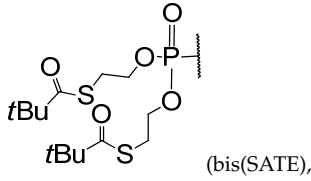
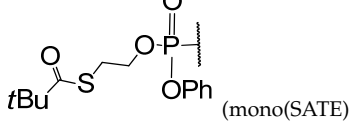
Entry ^a /DRD Approach, Structure and Number of Compounds Examined	Effective Concentration Value ^b ; Cell Line; Virus Variant (If Given) Cytotoxic Concentration Value ^c ; Cell Line Selectivity Index ^d (SI, If Given)	Ref.		
2.27/A ^e		maribavir	EC ₅₀ 3000 ± 131 nM; Vero E6; Omicron B.1.1.529/BA.5 CC ₅₀ > 100 μM; Vero E6 (3 virus variants evaluated)	[63–65]
2.28/A		nelarabine: R ¹ = OMe, R ² = NH ₂ vidarabine: R ¹ = NH ₂ , R ² = H	nelarabine: EC ₅₀ 1656 ± 71 nM; Vero E6; Omicron B.1.1.529/BA.5 CC ₅₀ > 100 μM; Vero E6 (3 virus variants evaluated)	[63–65]
2.29/A		5-azacytidine	EC ₅₀ 2.63 μM; Calu-3; Wuhan/WIV04/2019 CC ₅₀ 25.40 μM; Calu-3 SI 9.66	[67]
2.30/A/B ^e		azvudine: R = H  CL-236: R =	CL-236: EC ₅₀ 1.2 μM; Calu-3; BetaCoV/Wuhan/WIV04/2019 CC ₅₀ > 102.4 μM; Calu-3 SI 83	[68–70]
2.31/A/D ^e	 <p data-bbox="312 1469 663 1570">R² = Me, vinyl, ethynyl, cyclopropyl, furan-2-yl, thiophen-2-yl, Ph, benzofuran-2-yl, benzothiophen-2-yl, naphthalen-2-yl</p>  <p data-bbox="312 1671 663 1693">R² = H, (proTide),</p>  <p data-bbox="520 1850 624 1883">(bis(SATE)),</p>  <p data-bbox="536 1984 663 2018">(mono(SATE)) (25 compounds)</p>	R ¹ = H, R ² = furan-2-yl: EC ₅₀ 0.1 ± 0.03 μM; Huh7; hCoV-19/Czech Republic/NRL_6632_2/2020 CC ₅₀ 11 ± 2.5 μM; Huh7	[71]	

Table 2. Cont.

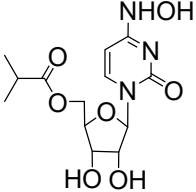
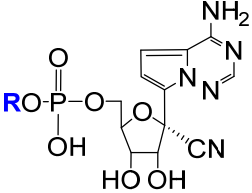
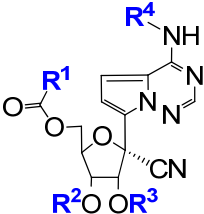
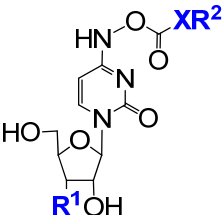
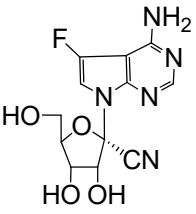
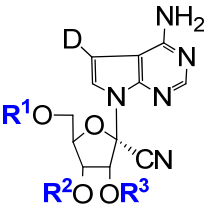
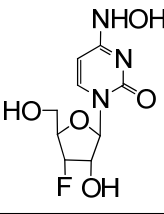
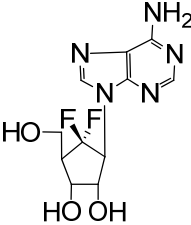
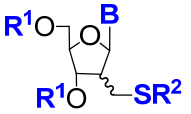
Entry ^a /DRD Approach, Structure and Number of Compounds Examined	Effective Concentration Value ^b ; Cell Line; Virus Variant (If Given) Cytotoxic Concentration Value ^c ; Cell Line Selectivity Index ^d (SI, If Given)	Ref.		
2.32/B		molnupiravir	EC ₅₀ 0.10 μM; <i>Calu-3</i> ; WA1 CC ₅₀ > 50 μM; <i>Calu-3</i> SI > 500	[36,54]
2.33/B ^e		R = 4-oxaicosan-1-yl, 3-oxahenicosan-1-yl, 2-OBn-4-oxadocosan-1-yl	R = 2-OBn-4-oxadocosan-1-yl: EC ₅₀ 0.14 μM; <i>Vero E6</i> ; USA-WA1/2020 CC ₅₀ 97.9 μM; <i>Vero E6</i> SI 699	[72,73]
2.34/B ^e		R ¹ = alkyl, cycloalkyl, CF ₃ CH ₂ , C ₆ H ₅ , α-aminoalkyl R ² , R ³ , R ⁴ = H, acetyl, isobutyryl (21 compounds)	obeldesivir (ATV006, R ¹ = isopropyl; R ² , R ³ , R ⁴ = H): EC ₅₀ 0.106 μM; <i>Vero E6</i> ; Omicron, B.1.1.529 CC ₅₀ 128.00 μM; <i>Vero E6</i> SI 1207.55 (4 virus variants evaluated)	[74]
2.35/B		X = O or CH ₂ R ¹ = OH or F R ² = C ₁₀ H ₂₁ , C ₁₂ H ₂₃ , C ₁₄ H ₂₉ (5 compounds)	X = CH ₂ , R = C ₁₄ H ₂₉ : EC ₅₀ 0.31 μM; <i>Vero</i> ; B1.1 529 BA.1 (Omicron); CC ₅₀ 6.32 μM; <i>Vero</i> (5 virus variants evaluated)	[75]
2.36/C			EC ₅₀ 3.30 μM; <i>Vero E6</i> (2 virus strains evaluated)	[53]
2.37/C ^e		R ¹ , R ² , R ³ = H or isobutyryl (4 compounds)	VV116 (R ¹ , R ² , R ³ = isobutyryl; hydrobromide): EC ₅₀ 0.35 ± 0.09 μM; <i>Vero E6</i> CC ₅₀ 289.19 ± 15.39 μM; <i>Vero E6</i> (2 virus variants evaluated)	[53]
2.38/C			EC ₅₀ 29.91 μM; <i>Vero</i> ; B1.1 529 BA.1 (Omicron); CC ₅₀ > 100 μM; <i>Vero</i> (5 virus variants evaluated)	[75]

Table 2. Cont.

Entry ^a /DRD Approach, Structure and Number of Compounds Examined	Effective Concentration Value ^b ; Cell Line; Virus Variant (If Given) Cytotoxic Concentration Value ^c ; Cell Line Selectivity Index ^d (SI, If Given)	Ref.		
2.39/D		EC ₅₀ ~2 μM; <i>Calu-3</i> CC ₅₀ > 25 μM; <i>Calu-3</i> SI > 12 μM	[47]	
2.40/D		B = thymine-1-yl, uracil-1-yl, N ⁶ -DMTr-adenine-1-yl R ¹ = TBDMS or (iPr) ₂ Si-O-Si(iPr) ₂ R ² = C ₄ H ₉ , Ac, pyranose-1-yl (11 compounds)	B = thymine-1-yl, R ¹ = (iPr) ₂ Si-O-Si(iPr) ₂ , <i>ara</i> R ² = C ₄ H ₉ ; EC ₅₀ 17 μM; <i>Vero E6</i> ; MOI 0.05 CC ₅₀ 16.6 μM; <i>Vero E6</i>	[76]

Approach A: repurposing of known NAs, including approved drugs or their prodrugs. Approach B: development of prodrugs of known anti-HCoV NAs. Approach C: structural modifications of the anti-HCoV NAs, leading to their nonprodrug analogs. Approach D: development of de novo-designed NAs. ^a Entry numbers include the number of the table and the position of a compound (or a group of compounds) on the timeline, taking into account the year of publication of the references discussed. ^b Exemplified as the effective compound concentration (EC₅₀ or EC₉₀ or IC₅₀). ^c Exemplified as the cytotoxic compound concentration (CC₅₀). ^d Defined as a ratio of the compound cytotoxic concentration and the compound effective concentration. Only values explicitly given by the authors are cited. ^e See text for details.

Uemura et al. examined the in vitro activity of tubercidin and its derivatives against SARS-CoV-2 (entries 2.14–2.16), HCoV-OC43 (entries 4.12–4.14), and HCoV-229E (entries 5.8–5.10) [56]. Four of the tested compounds showed submicromolar activity: tubercidin, 5-hydroxymethyltubercidin, 5-((hydroxyimino)methyl)tubercidin, and 5-nitrotubercidin. However, only 5-hydroxymethyltubercidin exhibited both advantageous activity and relatively low cytotoxicity (entries 2.14, 4.13, and 5.9). 5-Hydroxymethyltubercidin inhibited the replication of the examined viruses in a dose-dependent manner. Further experiments employing ZIKV RdRp suggested that 5-hydroxymethyltubercidin was incorporated into viral RdRp and inhibited the synthesis of the viral RNA by chain termination [56].

Sangivamycin is a natural nucleoside analog endowed with anticancer, antibiotic, and antiviral activity. Recently, the anti-SARS-CoV-2 properties of sangivamycin were reported by Bennett et al. (entry 2.22) [60]. When in vitro assayed against eight variants of SARS-CoV-2, IC₅₀ values in the low nanomolar range (14–82 nM) with the highest SI value > 39.0 for the B.1.1.7 (Alpha) variant in *Vero E6/TMPRSS2* cells were obtained. The activity of sangivamycin was cell-dependent but significantly lower than that of remdesivir found in the same experiments in all the host cells employed (*Vero* cells, *Caco-2* cells, and *Calu-3* cells). These preliminary studies showed an additive effect of sangivamycin and remdesivir. The mechanism of action of sangivamycin was not established. Tonix Pharmaceuticals announced that it would develop sangivamycin for the treatment of COVID-19 [77], emphasizing its good tolerability in patients subjected to the previous clinical trials [60].

Studies on cordycepin (3'-deoxyadenosine, entry 2.23) were triggered by a recently published in silico computational docking approach [78]. The results of this simulation strongly suggested that cordycepin interacted with the SARS-CoV-2 RNA-dependent RNA polymerase (RdRp). Indeed, it was shown that cordycepin strongly inhibited virus multiplication in vitro, with potency comparable to that of remdesivir [61]. Rabie proposed that the mechanism of inhibition of virus replication originated from the similarity of cordycepin and adenosine. During viral replication, cordycepin triphosphate was incorporated instead of adenosine triphosphate into the virus RNA by the RdRp. This incorporation

resulted in errors in the viral genetic code. As a consequence, a large number of mutations occurred (lethal mutagenesis). In a series of follow-up papers by Rabie and coworkers, using the nucleoside analogism approach, didanosine (2',3'-dideoxyinosine, entry 2.24) [62], riboprine, tecadenoson (entry 2.25) [63–66], forodesine (entry 2.26) [63–66], and maribavir (entry 2.27) [63–65] were studied and found to strongly inhibit the replication of SARS-CoV-2. The in silico computational study suggested that these NAs are strongly bound to the main active site of the RdRp molecule or to the 3'-to-5' exoribonuclease.

Azvodine (entry 2.30, R = H) is the first Chinese oral anti-COVID-19 drug [70,79]. This compound is almost inactive in vitro, but it is intracellularly phosphorylated to the triphosphate that displays broad-spectrum activity by inhibiting the SARS-CoV-2 RdRp. For research purposes, in order to better investigate the activity in vitro, a monophosphate prodrug of azvodine, CL-236 (entry 2.30), was also synthesized and tested. Conventional experiments proved the anticoronavirus properties of CL-236 (see also Table 4, entry 4.15) [69]. The distribution and phosphorylation in vivo of azvodine, as well as its metabolic pathway, were investigated in rats. While azvodine was detectable after oral administration in all tested organs, its triphosphate was observed only in the thymus. The clinical benefits of azvodine were demonstrated in experiments with infected rhesus macaques. The efficacy and safety of azvodine in patients with mild and common COVID-19 were evaluated in a clinical trial in China (ChiCTR2000029853) [68].

Lipid prodrugs of GS-441524 were developed as potential alternatives to remdesivir in order to overcome its metabolic instability (entry 2.33) [72]. The most active prodrug (R = 2-OBn-4-oxadocosan-1-yl) showed activity against two HCoV-2 (SARS-CoV-2, entry 2.33; and HCoV-229E, entry 5.12) and a variety of RNA viruses with excellent SIs ranging from 295 to 699 [72,73]. The active compound showed cell-dependent activity against SARS-CoV-2. It was significantly higher than that of remdesivir in *Vero* cells and equivalent to that of remdesivir in *PSC-human lung* cells, *Calu-3* cells, *Huh7.5* cells, and *Caco-2* cells. In vivo studies revealed the stability of this compound in plasma for 24 h and its good tolerability during a 7-day treatment (Syrian hamsters). In contrast, the prodrug (R = 2-OBn-4-oxadocosan-1-yl) was less active against HCoV-229E than remdesivir.

Among the 21-member set of mono-, di-, tri-, or tetraacylated derivatives of GS-441524 (entry 2.34), Cao et al. identified the 5'-O-esters (R¹,R² = H, R³ = prop-2-yl, prop-1-yl, oct-1-yl, pent-3-yl, phenyl, 2-methylprop-1-yl) as endowed with higher in vitro replicon activity against SARS-CoV-2 [EC₅₀ 0.217 μM (R³ = prop-1-yl) – 0.521 (R³ = prop-2-yl) μM] than the parent GS-441524 (EC₅₀ 0.955 μM, HEK 293T cells) [74]. Moreover, the isobutyric acid ester (R³ = prop-2-yl, obeldesivir) and the nonanoic acid ester (R³ = oct-1-yl) showed higher in vitro activity than GS-441524 or remdesivir against the selected variants of SARS-CoV-2 in *Vero E6* cells. However, only obeldesivir featured a satisfactory SI (1207.55, Omicron variant in *Vero E6* cells). It met standards as an oral drug candidate because, compared with the parent GS-441524, it (a) featured acceptable water solubility (686.02 μg/mL), (b) reached higher oral bioavailability in animal models (macaques, about 30% vs. 8.3%, respectively), (c) achieved a broad distribution in the major target organs (C57BL/6 mice) for SARS-CoV-2 infection, and (d) showed potent anti-SARS-CoV-2 efficacy in different mouse models. Currently, obeldesivir is under clinical trials in participants that have a high risk of getting a serious COVID-19 illness (ClinicalTrials.gov Identifier: NCT05603143).

Xie et al. synthesized several derivatives of GS-441524 by introducing halogen, hydroxyl, or cyano groups at the purine 7-position (entry 2.36) [53]. Further modifications involved deuterated analogs, which, due to some synthetic problems, were obtained only at the 7-position. In this way, the compound VV116 (entry 2.37) was identified as a promising candidate. It was used as a hydrobromide salt for its stability and improved bioavailability compared to the other compounds in the series. When orally administered in mice, it showed dose-dependent efficacy. A phase 3 observer-blinded, randomized trial showed that VV116 was noninferior to paxlovid (recommended by the World Health Organization for treating mild-to-moderate COVID-19) with respect to the time to sustained clinical recovery and had fewer safety concerns [80].

Hocek and coworkers evaluated a broad panel of 7-substituted 7-deazapurine ribonucleosides, monophosphate prodrugs, and triphosphates against emerging RNA viruses, including SARS-CoV-2 (entry 2.31) [71]. The nucleosides ($R^1 = H$) containing $R^2 =$ ethynyl, furany-2-yl, benzofurany-2-yl, benzothiophen-2-yl, or naphthalen-2-yl showed micromolar or submicromolar anti-SARS-CoV-2 activity in vitro and relatively low toxicity to the host *Huh7* cells. Their prodrugs ($R^1 =$ proTide, mono(SATE) or bis(SATE)) were comparable ($R^1 =$ bis(SATE), $R^2 =$ benzofurany-2-yl) or less active in these assays. Comparative studies on the parent nucleoside ($R^1 = H$, $R^2 =$ benzofurany-2-yl) and its prodrugs ($R^1 =$ proTide or bis(SATE)) showed that the bis(SATE) prodrug ($R^1 =$ bis(SATE)) was the best form for the cellular membrane transport and intracellular release of the nucleoside monophosphate ($R^1 = P(O)(OH)O^-$, $R^2 =$ benzofurany-2-yl) (*Huh7* cells). In light of these observations, the comparable or somewhat lower in vitro activity of this prodrug than that of its parent nucleoside ($R^1 = H$, $R^2 =$ benzofurany-2-yl) was suggested to be due to the plausible alternative mechanisms of action of the nucleoside ($R^1 =$ bis(SATE), $R^2 =$ benzofurany-2-yl), which might not involve activation through phosphorylation.

1.3. The Nucleoside Analogs Evaluated as In Vitro Inhibitors of MERS-CoV Replication

In general, the number of reported studies on NAs as potential inhibitors of MERS-CoV replication (Table 3) is much smaller than the number of those focused on SARS-CoV or SARS-CoV-2. The majority of these studies dealt with the repurposing of known NAs (approach A, entries 3.1–3.9). Among these compounds, NHC (entry 3.1) and remdesivir (entry 3.5) showed the highest activity in vitro with good SI values. The 6'-fluorinated analogs of (–)-aristeromycin (entry 3.10) are the only de novo-designed NAs. They showed promising one-digit micromolar activities, although accompanied by appreciable cytotoxicity (for details, see also entry 1.38).

Table 3. The nucleoside analogs evaluated in vitro against replication of MERS-CoV.

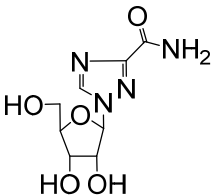
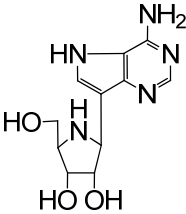
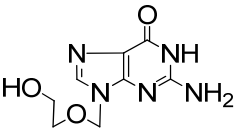
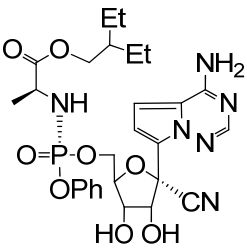
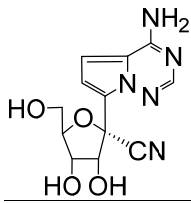
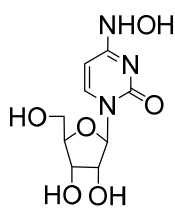
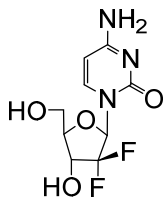
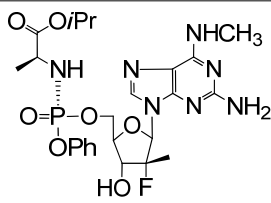
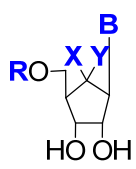
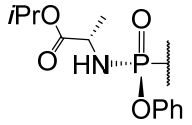
Entry ^a /DRD Approach, Structure, and Number of Compounds Examined	Effective Concentration Value ^b ; Cell Line; Virus Variant (If Given) Cytotoxic Concentration Value ^c ; Cell Line Selectivity Index ^d (SI, If Given)	Ref.
3.1/A 	ribavirin IC ₅₀ 9.99 ± 2.97 µg/mL; <i>Vero</i> CC ₅₀ > 1660 µg/mL; <i>Vero</i> SI > 152.98	[81]
3.2/A ^e 	galidesivir (BCX4430, immucillin-A) EC ₅₀ 68.4 µM; <i>Vero E6</i> ; Jordan N3 CC ₅₀ > 100 µM; <i>Vero E6</i> SI > 1.5	[40]
3.3/A 	$R^1 = H, Me$ $R^2 = NH_2$ (3 compounds) $R^1 = Me, R^2 = NH_2$: EC ₅₀ 23 ± 0.6 µM; <i>Vero</i> ; EMC/2012 CC ₅₀ 71 ± 14 µM; <i>Vero</i>	[41]
3.4/A 	acyclovir EC ₅₀ > 1000 µM; <i>Vero</i> ; EMC/2012 CC ₅₀ > 1000 µM; <i>Vero</i>	[41]

Table 3. Cont.

Entry ^a /DRD Approach, Structure, and Number of Compounds Examined	Effective Concentration Value ^b ; Cell Line; Virus Variant (If Given) Cytotoxic Concentration Value ^c ; Cell Line Selectivity Index ^d (SI, If Given)	Ref.	
3.5/A	 remdesivir	EC ₅₀ 0.34 μM; Vero CC ₅₀ > 20 μM; Vero IC ₅₀ 0.025 μM; Calu-3 CC ₅₀ > 10 μM; Calu-3 SI > 400 IC ₅₀ 0.074 ± 0.023 μM; HAE CC ₅₀ > 10 μM; HAE SI > 100	[82] [42] [42,43]
3.6/A	 GS-441524	IC ₅₀ 0.86 ± 0.78 μM; HAE CC ₅₀ > 100 μM; HAE	[42,43]
3.7/A	 NHC	IC ₅₀ 0.56 μM; DBT-9 CC ₅₀ > 200 μM; DBT-9 IC ₅₀ 0.024 μM; HAE; RFP (2 virus variants evaluated)	[83] [36]
3.8/A	 gemcitabine	EC ₅₀ 1.216 μM; Vero E6	[39]
3.9/A	 AT-511 (bemnifosbuvir, free form of AT-527)	EC ₉₀ 37 ± 28 μM; Huh7 CC ₅₀ > 86 μM; Huh7 SI > 3.3	[44]
3.10/D	 X = H or F Y = H or F B = uracil-1-yl, cytosin-1-yl, adenin-1-yl, N ⁶ -Me-adenin-1-yl, R = H or  (14 compounds)	X,Y = F, B = adenin-1-yl, R = H: EC ₅₀ 0.2 μM; Vero E6; EMC/2012 CC ₅₀ 3.2 μM; Vero E6 SI 16	[47,51]

Approach A: repurposing of known NAs, including approved drugs or their prodrugs. Approach D: development of the de novo-designed NAs. ^a Entry numbers include the number of the table and the position of a compound (or a group of compounds) on the timeline, taking into account the year of publication of the references discussed. ^b Exemplified as the effective compound concentration (EC₅₀ or EC₉₀ or IC₅₀). ^c Exemplified as the cytotoxic compound concentration (CC₅₀). ^d Defined as the ratio of the compound cytotoxic concentration and the compound effective concentration. Only values explicitly given by the authors are cited. ^e See text for details.

1.4. The Nucleoside Analogs Evaluated as In Vitro Inhibitors of HCoV-OC43 Replication

The number of studies on the potential of NAs to inhibit the replication of HCoV-OC43 is relatively limited (Table 4). All assays found in the literature featured repurposed known NAs (approach A, entries 4.1–4.14), with CL-236 (the prodrug of azvudine, approach B) as the only exception (entry 4.15, for details see also entry 2.30). Among the repurposed compounds, remdesivir was reported to show high activity in vitro (entry 4.1), although accompanied by considerable cytotoxicity in *Huh7* cells. The compounds NHC (entry 4.2), AT-511 (entry 4.11), and 7-hydroxymethyltubercidin (entry 4.13; for details, see also entry 2.14) displayed submicromolar activities and relatively high SI values ranging from 100 (NHC) to >170 (AT-511). Lamivudine and emtricitabine are the only examples of noncanonical L-nucleosides among the repurposed NAs (entry 4.8).

Table 4. The nucleoside analogs evaluated in vitro against the replication of HCoV-OC43.

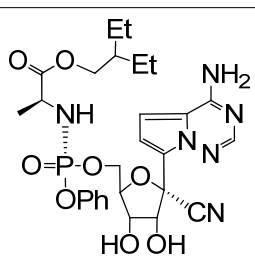
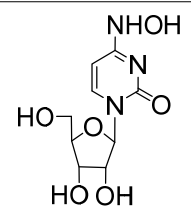
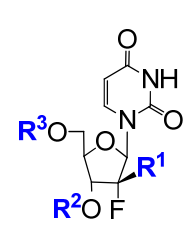
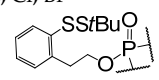
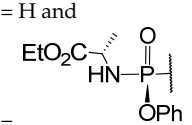
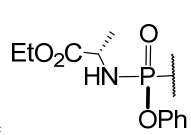
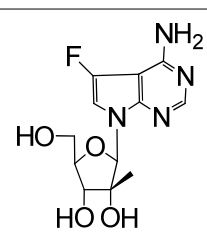
Entry ^a /DRD Approach, Structure, and Number of Compounds Examined	Effective Concentration Value ^b ; Cell Line; Virus Variant (If Given) Cytotoxic Concentration Value ^c ; Cell Line Selectivity Index ^d (SI, If Given)	Ref.	
4.1/A 	remdesivir EC ₅₀ 0.04 ± 0.1 μM <i>Huh7</i> CC ₅₀ 2.1 μM; <i>Huh7</i> SI 52	[52]	
4.2/A 	NHC EC ₅₀ 0.8 ± 0.03 μM; <i>Huh7</i> CC ₅₀ 80.3 μM; <i>Huh7</i> SI 100	[52]	
4.3/A 	R ¹ = Me, Cl, Br R ² , R ³ =  or R ² = H and  R ³ = (4 compounds)	 EC ₅₀ 5.9 ± 0.6 μM; <i>Huh7</i> CC ₅₀ > 100 μM; <i>Huh7</i>	[52]
4.4/A 	EC ₅₀ 6.7 ± 1.1 μM; <i>Huh7</i> CC ₅₀ 38 μM; <i>Huh7</i>	[52]	

Table 4. Cont.

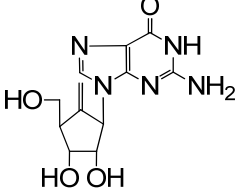
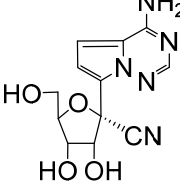
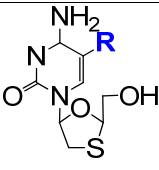
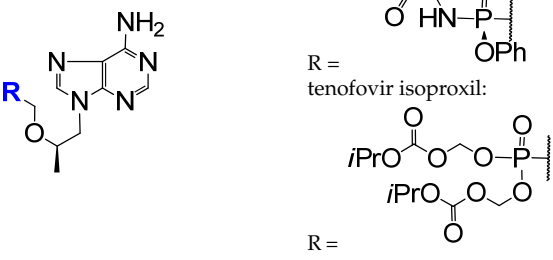
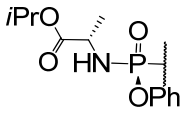
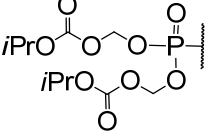
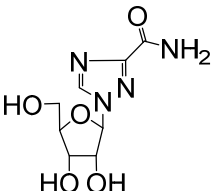
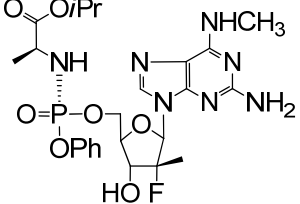
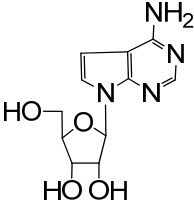
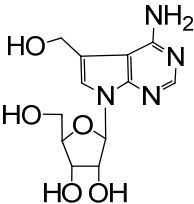
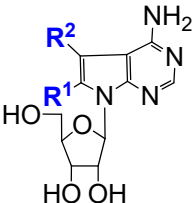
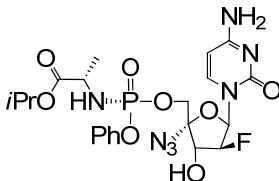
Entry ^a /DRD Approach, Structure, and Number of Compounds Examined	Effective Concentration Value ^b ; Cell Line; Virus Variant (If Given) Cytotoxic Concentration Value ^c ; Cell Line Selectivity Index ^d (SI, If Given)	Ref.	
4.5/A	 <p>2'-MeC: R¹ = H, R² = OH, R³ = Me ALS-8112: R¹ = CH₂Cl, R² = F, R³ = H</p>	2'-MeC: EC ₅₀ 10 ± 0.7 μM; <i>Huh7</i> CC ₅₀ > 100 μM; <i>Huh7</i>	[52]
4.6/A	 <p>entecavir</p>	EC ₅₀ > 20 μM; <i>Vero</i> CC ₅₀ > 20 μM; <i>Vero</i>	[52]
4.7/A	 <p>GS-441524</p>	EC ₅₀ > 10 μM; <i>Vero</i> CC ₅₀ 13.2 ± 0.8 μM; <i>Vero</i>	[52]
4.8/A	 <p>lamivudine: R = H emtricitabine: R = F</p>	Lamivudine and emtricitabine: EC ₅₀ > 20 μM; <i>Vero</i> CC ₅₀ > 20 μM; <i>Vero</i>	[52]
4.9/A	 <p>tenofovir alafenamide: R =  tenofovir isoproxil: R = </p>	EC ₅₀ > 20 μM; <i>Vero</i> CC ₅₀ > 20 μM; <i>Vero</i>	[52]
4.10/A	 <p>ribavirin</p>	EC ₅₀ 20.6 μM; <i>Huh7</i> CC ₅₀ 22.1 μM; <i>Huh7</i>	[52]
4.11/A	 <p>AT-511 (bemnifosbuvir, free form of AT-527)</p>	EC ₉₀ 0.5 μM; <i>Huh7</i> CC ₅₀ > 86 μM; <i>Huh7</i> SI > 170 (2 virus variants evaluated)	[44]

Table 4. Cont.

Entry ^a /DRD Approach, Structure, and Number of Compounds Examined	Effective Concentration Value ^b ; Cell Line; Virus Variant (If Given) Cytotoxic Concentration Value ^c ; Cell Line Selectivity Index ^d (SI, If Given)	Ref.
4.12/A 	tubercidin EC ₅₀ 0.11 μM; MRC5 CC ₅₀ 0.66 μM; MRC5	[56]
4.13/A 	5-hydroxymethyltubercidin EC ₅₀ 0.378 ± 0.023 μM; MRC5 CC ₅₀ > 50 μM; MRC5 SI > 132	[56]
4.14/A 	R ¹ = H or CN R ² = H, CH=NOH, NO ₂ Me, CN (5 compounds) R ¹ = H, R ² = CH=NOH: EC ₉₀ 0.055 μM; MRC5 CC ₅₀ 0.74 μM; MRC5	[56]
4.15/B 	CL-236 EC ₅₀ 1.2 μM; H460; VR1558 SI 20	[68]

Approach A: repurposing of known NAs, including approved drugs or their prodrugs. Approach B: development of prodrugs of known anti-HCoV NAs. ^a Entry numbers include the number of the table and the position of a compound (or a group of compounds) on the timeline, taking into account the year of publication of the references discussed. ^b Exemplified as the effective compound concentration (EC₅₀ or EC₉₀). ^c Exemplified as the cytotoxic compound concentration (CC₅₀). ^d Defined as the ratio of the compound cytotoxic concentration and the compound effective concentration. Only values explicitly given by the authors are cited.

1.5. The Nucleoside Analogs Evaluated as In Vitro Inhibitors of HCoV-229E Replication

The number of reports on nucleoside inhibitors of HCoV-229E is rather limited (Table 5). The repurposing of known NAs (approach A, entries 5.1–5.11) or the examination of prodrugs of known anti-HCoV NAs (approach B, entry 5.12) were the major DRD approaches. Besides remdesivir (entry 5.1) and the compound AT-511 (entry 5.7), the derivatives of tubercidin (entries 5.8–5.10, for details, see also entries 2.10 and 2.14–2.16) and the 5'-O-lipid prodrugs of GS-441524 (entry 5.12, for details, see also 2.34) showed promising submicromolar activities. Among them, 7-hydroxymethyltubercidin featured the highest SI value (entry 5.9, SI > 94). The de novo-designed nucleoside analogs (approach D) were the 1,2,3-triazole NAs (entry 5.13) and the 2'-branched nucleosides (entry 5.14). These compounds showed moderate anti-HCoV-229E activity and suffered from appreciable cytotoxicity towards the host HEL cells.

Parang and coworkers compared the anti-HCoV-229E activity of remdesivir (entry 5.1) with known anti-HIV agents, such as alovudine, lamivudine, islatravir, emtricitabine, or tenofovir, and their derivatives (entries 5.2–5.6) [84]. Among the tested compounds, only remdesivir exhibited significant activity. These findings were tentatively explained by the

unique interaction of remdesivir with the RdRp of coronaviruses compared to the mode of action of anti-HIV drugs that interfere with the reverse transcriptase.

Table 5. The nucleoside analogs evaluated in vitro against the replication of HCoV-229E.

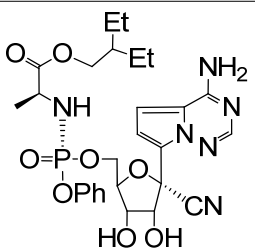
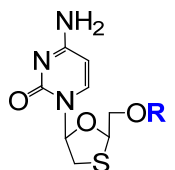
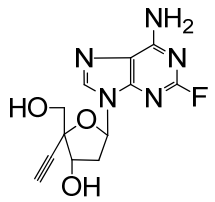
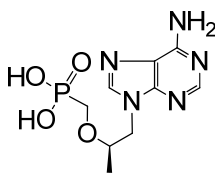
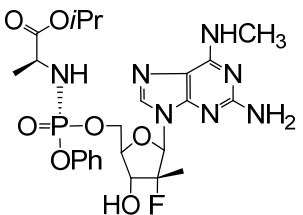
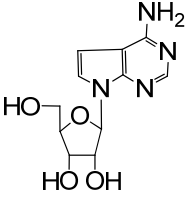
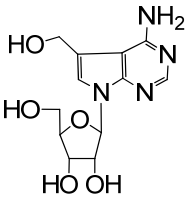
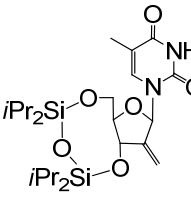
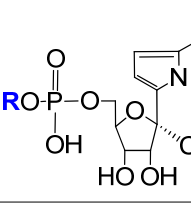
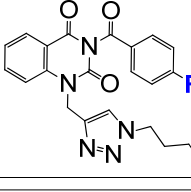
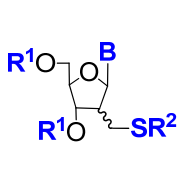
Entry ^a /DRD Approach, Structure, and Number of Compounds Examined	Effective Concentration Value ^b ; Cell Line; Virus Variant (If Given) Cytotoxic Concentration Value ^c ; Cell Line Selectivity Index ^d (SI, If Given)	Ref.	
5.1/A ^e 	remdesivir	EC ₅₀ 0.07 μM; MRC5 TC ₅₀ > 2.0 μM; MRC5 SI > 28.6	[84]
5.2/A 	R = H (alovudine) or CH ₃ CH ₂ S(CH ₂) ₁₁ C(O)-	R = CH ₃ CH ₂ S(CH ₂) ₁₁ C(O)-: EC ₅₀ > 45.4 μM; MRC5 TC ₅₀ 45.4 μM; MRC5	[84]
5.3/A 	R = H (lamivudine) or CH ₃ (CH ₂) ₁₂ C(O)-	R = CH ₃ (CH ₂) ₁₂ C(O)-: EC ₅₀ > 47.5 μM; MRC5 TC ₅₀ 47.5 μM; MRC5	[84]
5.4/A 	islatravir	EC ₅₀ > 55.3 μM; MRC5 TC ₅₀ 55.3 μM; MRC5	[84]
5.5/A 	R = H (emtricitabine) or CH ₃ (CH ₂) ₁₂ C(O)-	R = CH ₃ (CH ₂) ₁₂ C(O)-: EC ₅₀ 87.5 μM; MRC5 TC ₅₀ 72.8 μM; MRC5 SI 1.2	[84]
5.6/A 	tenofovir	EC ₅₀ > 100 μM; MRC5 TC ₅₀ > 100 μM; MRC5	[84]
5.7/A 	AT-511 (bemnifosbuvir, free form of AT-527)	EC ₅₀ 1.8 ± 0.3 μM; BHK-21 CC ₅₀ > 100 μM; BHK-21 SI > 55 (2 virus variants evaluated)	[44]

Table 5. Cont.

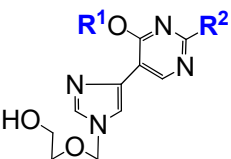
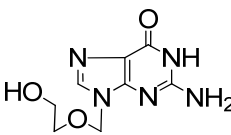
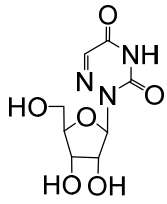
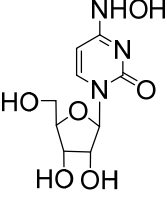
Entry ^a /DRD Approach, Structure, and Number of Compounds Examined	Effective Concentration Value ^b ; Cell Line; Virus Variant (If Given) Cytotoxic Concentration Value ^c ; Cell Line Selectivity Index ^d (SI, If Given)	Ref.
5.8/A 	tubercidin EC ₅₀ < 0.078 μM; MRC5 CC ₅₀ 0.66 μM; MRC5	[56]
5.9/A 	5-hydroxymethyltubercidin EC ₅₀ 0.528 ± 0.029 μM; MRC5 CC ₅₀ > 50 μM; MRC5 SI > 94	[56]
5.10/A 	R ¹ = H or CN R ² = H, CH=NOH, NO ₂ Me, CN(5 compounds) R ¹ = H, R ² = CH=NOH: EC ₅₀ < 0.078 μM; MRC5 CC ₅₀ 0.74 μM; MRC5	[56]
5.11/A 	EC ₅₀ 4.0 μM; HEL CC ₅₀ 10 μM; HEL	[76]
5.12/B 	R = 4-oxaicosan-1-yl, 3-oxahenicosan-1-yl, 2-OBn-4-oxadocosan-1-yl R = 2-OBn-4-oxadocosan-1-yl: EC ₅₀ 0.15 μM; MRC5 CC ₅₀ > 50 μM; MRC5	[72]
5.13/D 	R = H or F R = H: EC ₅₀ 18.5 ± 13.5 μM; HEL MCC > 20 μM; HEL	[85]
5.14/D 	B = thymine-1-yl, uracil-1-yl, N ⁶ -DMTr-adenine-1-yl R ¹ = TBDMS or (iPr) ₂ Si-O- Si(iPr) ₂ R ² = C ₄ H ₉ , Ac, pyranos-1-yl (11 compounds) B = uracil-1-yl, R ¹ = (iPr) ₂ Si-O-Si(iPr) ₂ , araR ² = C ₄ H ₉ : EC ₅₀ 4.1 μM; HEL CC ₅₀ 10 μM; HEL	[76]

Approach A: repurposing of known NAs, including approved drugs or their prodrugs. Approach B: development of prodrugs of known anti-HCoV NAs. Approach D: development of de novo-designed NAs. ^a Entry numbers include the number of the table and the position of a compound (or a group of compounds) on the timeline, taking into account the year of publication of the references discussed table. ^b Exemplified as the effective compound concentration (EC₅₀). ^c Exemplified as the cytotoxic compound concentration (CC₅₀ or TC₅₀ or MCC). ^d Defined as the ratio of the compound cytotoxic concentration and the compound effective concentration. Only values explicitly given by the authors are cited. ^e See text for details.

1.6. The Nucleoside Analogs Evaluated as In Vitro Inhibitors of HCoV-NL63 Replication

We found two original studies that examined the potential of the repurposed NAs to inhibit the replication of HCoV-NL63 in vitro (Table 6, approach A). Saley-Radke and coworkers identified flexible analogs of acyclovir (entry 6.1) as moderately active in *Vero 118* cells. Compared with inactive acyclovir (entry 6.2), these results confirmed the hypothesis of biological benefits resulting from introducing an additional rotatable bond into the nucleoside molecule. 6-azauridine and NHC (entries 6.3 and 6.4, respectively) showed significant nanomolar activity, with 6-azauridine having a very high SI value (2500).

Table 6. The nucleoside analogs evaluated in vitro against the replication of HCoV-NL63.

Entry ^a /DRD Approach, Structure, and Number of Compounds Examined	Effective Concentration Value ^b ; Cell Line; Virus Variant (If Given)	Cytotoxic Concentration Value ^c ; Cell Line	Ref.	
		Selectivity Index ^d (SI, If Given)		
6.1/A		R ¹ = H, Me R ² = NH ₂ (3 compounds)	R ¹ = Me, R ² = NH ₂ : EC ₅₀ 8.8 ± 1.5 μM; <i>Vero 118</i> ; clinic isolate CC ₅₀ 120 ± 37 μM; <i>Vero 118</i>	[41]
6.2/A		acyclovir	EC ₅₀ > 100 μM; <i>Vero 118</i> ; clinic isolate CC ₅₀ > 100 μM; <i>Vero 118</i>	[41]
6.3/A		6-azauridine	IC ₅₀ 32 nM; <i>LLC-MK2</i> ; Amsterdam 1 CC ₅₀ 80 μM; <i>LLC-MK2</i> SI 2500	[86]
6.4/A		NHC	IC ₅₀ 400 nM; <i>LLC-MK2</i> ; Amsterdam 1 CC ₅₀ > 100 μM; <i>LLC-MK2</i> SI > 250	[86]

Approach A: repurposing of known NAs, including approved drugs or their prodrugs. ^a Entry numbers include the number of the table and the position of a compound (or a group of compounds) on the timeline, taking into account the year of publication of the references discussed. ^b Exemplified as the effective compound concentration (EC₅₀ or IC₅₀). ^c Exemplified as the cytotoxic compound concentration (CC₅₀). ^d Defined as the ratio of the compound cytotoxic concentration and the compound effective concentration. Only values explicitly given by the authors are cited.

1.7. The Nucleoside Analogs Evaluated as Inhibitors of HCoV-Related Enzymes

The NAs evaluated as potential inhibitors of HCoV-related enzymes are collected in Table 7. Two DRD approaches were employed to find active compounds: the repurposing of known NAs or their prodrugs (approach A, entries 7.1–7.10) or the development of de novo-designed NAs (approach D, entries 7.11–7.17). The NAs were evaluated as potential inhibitors of SARS-CoV (or SARS-CoV-2) nonstructural proteins, such as the RNA cap guanine-N7-methyltransferase (nsp14) or 2'-O-methyltransferase nsp16–nsp10 complex (nsp16–nsp10 complex) (entries 7.1, 7.6, and 7.11–7.16) and MERS-CoV nsp16–nsp10 complex (entry 7.2). Very recent studies by Vedadi and coworkers also involved nsp10–nsp16 complexes from HCoV-OC43, HCoV-HKU1, HCoV-NL63, HCoV-229E, and MERS-CoV as drug targets (entry 7.6). Owing to the structural relation between sinefun-

gin and AdoHcy (entry 7.1), the NAs evaluated as potential inhibitors of the RNA cap guanine-*N*7-methyltransferase nsp14 or 2'-*O*-methyltransferase nsp16–nsp10 complex are mostly the 6'-modified-5'-adenosyl amino acids (entry 7.6), 5'-adenosyl ureides (entry 7.6), bis-adenosyl conjugates (entry 7.11), deaza-analogs of AdoHcy (entry 7.12), or non-amino acid 5'-modified adenosines (entries 7.13–7.17). The 5'-deoxy-5'-sulfonamido-adenosines (entries 7.14–7.17) or their 7-deaza counterparts (entries 7.16 and 7.17) are a very broad group of compounds. Among the de novo-designed NAs (approach D), compounds with higher inhibitory activity towards SARS-CoV nsp14 (entry 7.12) or SARS-CoV nsp14 (entries 7.13, 7.14, and 7.16) than that of sinefungin were identified. These compounds are derivatives of 7-deaza-5'-deoxy-5'-sulfonamido-adenosine (entries 7.12, 7.14, and 7.16) or 5'-deoxy-5'-thio-adenosine (entry 7.13). Molecular docking was employed to identify the mechanism of action of these inhibitors (entries 7.6, 7.11–7.14, 7.16, and 7.17). Studies focused on SARS-CoV (or SARS-CoV-2) RdRp (entries 7.3–7.5, 7.8, and 7.9) or SARS-CoV-2 3C-like protease (3CL-Pro) (entry 7.7) were also reported.

Table 7. The nucleoside analogs assessed for their in vitro effect on HCoVs-related enzymes.

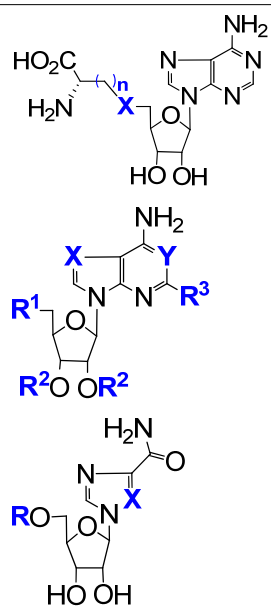
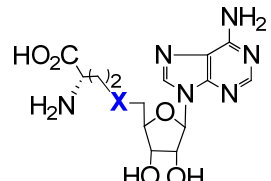
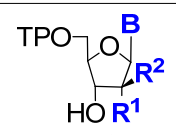
Entry ^a /DRD Approach, Structure and Number of Compounds Examined	Object of Study ^b Antiviral Effect(s) If Given ^c	Ref.	
7.1/A 	X = S or (S)-CH-NH ₂ n = 1 or 2 (3 compounds)	Inhibition of SARS-CoV nsp14 and SARS-CoV nsp16–nsp10 complex sinefungin (X = (S)-CH-NH ₂ , n = 2): IC ₅₀ 496 nM ± 18, nsp14 IC ₅₀ 736 nM ± 71; nsp16/nsp10 AdoHcy (X = S, n = 2): IC ₅₀ 16 μM ± 1.2, nsp14 IC ₅₀ 12 μM ± 1.9, nsp16/nsp10	[87,88]
7.2/A 	X = S (AdoHcy) or (S)-CH-NH ₂ (sinefungin)	Inhibition of MERS-CoV nsp16–nsp10 complex AdoHcy: IC ₅₀ 7 μM ± 0.4 sinefungin: IC ₅₀ 7.4 μM ± 0.9	[88,89]
7.3/A 	R ¹ = H, OH, Me, F R ² = H, OH, Me B = cytosin-1-yl, uracil-1-yl, adenin-9-yl, 3-carbamoyl-5-fluoro-2-oxopyrazin-1-yl, 3-carbamoyl-1H-1,2,4-triazol-1-yl (7 compounds)	Selectivity of the SARS-CoV-2 RdRp towards incorporation of the nucleoside analog triphosphate into viral RNA over a natural nucleotide. Low discrimination of the enzyme against the cytidine triphosphate derivative (B = cytosin-1-yl, R ¹ = F, R ² = H) over the reference cytidine triphosphate	[89,90]

Table 7. Cont.

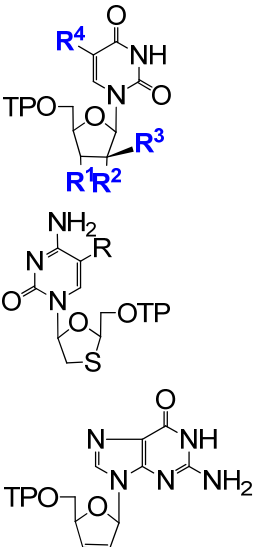
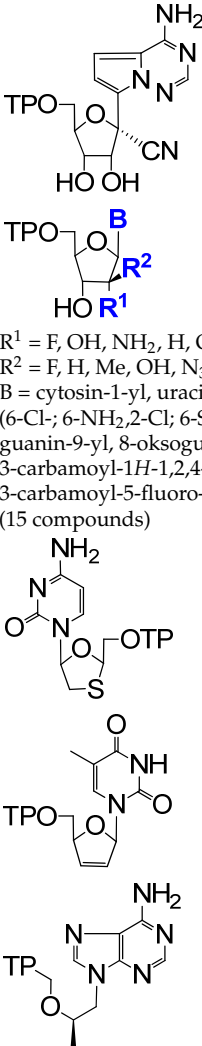
Entry ^a /DRD Approach, Structure and Number of Compounds Examined	Object of Study ^b Antiviral Effect(s) If Given ^c	Ref.	
7.4/A	 <p> $R^1 = \text{OH}, \text{N}_3, \text{F}$ $R^2 = \text{H or F}$ $R^3 = \text{H or Me}$ $R^4 = \text{H or Me}$ (3 compounds) </p> <p>triphosphate of lamivudine ($R = \text{H}$) or emtricitabine ($R = \text{F}$)</p> <p>carbovir triphosphate</p>	<p>Proclivity of SARS-CoV RdRp or SARS-CoV-2 RdRp to incorporate the nucleoside triphosphate into the virus RNA</p> <p>Sofosbuvir nucleoside triphosphate ($R^1 = \text{OH}, R^2 = \text{F}, R_3 = \text{Me}, R^4 = \text{H}$) was incorporated by the RdRp, terminated the polymerase reaction and was resistant to SARS-CoV-2 proofreader</p>	[90–93]
7.5/A	 <p>GS-441524 triphosphate</p> <p> $R^1 = \text{F}, \text{OH}, \text{NH}_2, \text{H}, \text{OMe}$ $R^2 = \text{F}, \text{H}, \text{Me}, \text{OH}, \text{N}_3$ $B = \text{cytosin-1-yl, uracil-1-yl, purin-9-yl}$ $(6\text{-Cl-}; 6\text{-NH}_2, 2\text{-Cl}; 6\text{-SMe}, 2\text{-NH}_2; 6\text{-SH}, 2\text{-NH}_2),$ $\text{guanin-9-yl, 8-oksoguanin-9-yl,}$ $3\text{-carbamoyl-1H-1,2,4-triazol-1-yl,}$ $3\text{-carbamoyl-5-fluoro-2-oxopyrazin-1-yl}$ (15 compounds) </p> <p>lamivudine triphosphate</p> <p>stavudine triphosphate</p> <p>tenofovir triphosphate</p>	<p>Incorporation of nucleotide analogs to viral RNA by SARS-CoV-2 RdRp</p> <p>The incorporation of GS-441524 triphosphate and delay in viral RNA chain termination</p>	[93,94]

Table 7. Cont.

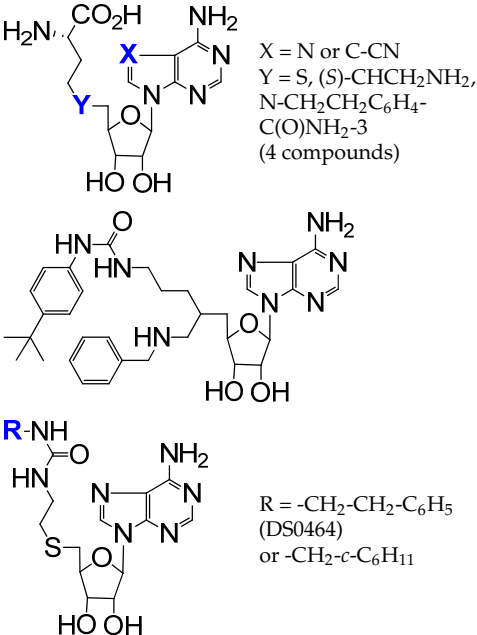
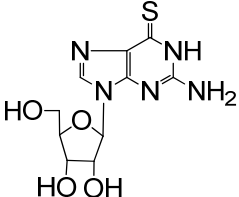
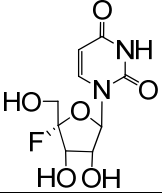
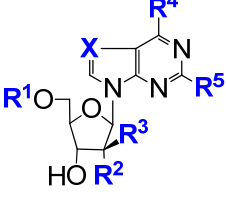
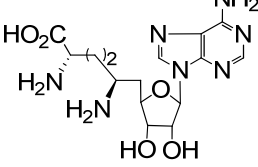
Entry ^a /DRD Approach, Structure and Number of Compounds Examined	Object of Study ^b Antiviral Effect(s) If Given ^c	Ref.	
7.6/A ^d	 <p>X = N or C-CN Y = S, (S)-CHCH₂NH₂, N-CH₂CH₂C₆H₄- C(O)NH₂-3 (4 compounds)</p> <p>R = -CH₂-CH₂-C₆H₅ (DS0464) or -CH₂-c-C₆H₁₁</p>	<p>Inhibition of SARS-CoV-2 nsp14, SARS-CoV-2 nsp10–nsp16 complex from SARS-CoV, SARS-CoV-2, HCoV-OC43, HCoV-HKU1, HCoV-NL63, HCoV-229E, and MERS-CoV and selectivity against 20 human protein lysine methyltransferases</p> <p>Compound SS148 (X = C-CN, Y = S): IC₅₀ 0.07 ± 0.006 μM; SARS-CoV-2 nsp14 IC₅₀ 0.2 ± 0.04 μM; HCoV-NL63 nsp10–nsp16 complex Compound WZ16 (X = N, Y = (S)-CH-CH₂NH₂): IC₅₀ 0.19 ± 0.04 μM; SARS-CoV-2 nsp14 IC₅₀ 2.5 ± 0.1 μM; SARS-CoV nsp10–nsp16 complex</p>	[94–96]
7.7/A ^d	 <p>thioguanosine</p>	<p>The inhibitory effect on SARS-CoV-2 3CL-Pro IC₅₀ 6.3 μM; SARS-CoV-2 3CL-Pro IC₅₀ 3.9 μM; SARS-CoV-2; Vero E6 CC₅₀ > 20, Vero E6</p>	[97]
7.8/A ^d	 <p>EIDD-2749</p>	<p>Inhibition of SARS-CoV-2 RdRp EC₅₀ 2.47 μM; HAE; USA-WA1/2020 CC₅₀ 467.9 μM; HAE</p>	[98]
7.9/A ^d	 <p>R¹ = H or -[P(O)(OH)O]₃H R², R³ = H or OH R⁴ = SH or NH₂ R⁵ = NH₂, F or H X = N or C-I (4 compounds)</p>	<p>Inhibition of SARS-CoV-2 RdRp R¹, R³, R⁵ = H, R² = OH, R⁴ = NH₂, X = C-I EC₅₀ 0.75 μM; SARS-CoV-2 RdRp CC₅₀ 59.46 μM; HEK 293T EC₅₀ 1.56 μM; HCoV-OC43; HCT-8 EC₅₀ 3.62 μM; HCoV-NL63; LLCM-K2</p>	[99]
7.10/A ^d	 <p>sinefungin</p>	<p>Disruption of WT SARS-CoV-2 nsp16 activity</p>	[100]

Table 7. Cont.

Entry ^a /DRD Approach, Structure and Number of Compounds Examined	Object of Study ^b Antiviral Effect(s) If Given ^c	Ref.	
7.11/D ^d		Inhibition of SARS-CoV nsp14 R = -S(O) ₂ -C ₆ H ₃ -3-NO ₂ ,4-Cl: IC ₅₀ 0.6 ± 0.1 μM	[101]
7.12/D ^d	<p>Ar = Ph, naphthyl, guinolin-3-yl, benzimidazol-2-yl, benzo[b]thiophen-5-yl X = CH₂, -CH₂-CH₂-, -C≡C- (8 compounds)</p>	Inhibition of SARS-CoV nsp14 R = guinolin-3-yl: IC ₅₀ 3 ± 0.5 nM	[102]
7.13/D ^d	<p>X = CH₂ or C(O) Y = S, NH, N(3°), 1,2,3-triazole, piperazine R = substituted alkyl, aryl, benzyl (36 compounds)</p>	Inhibition of SARS-CoV-2 nsp14, SARS-CoV-2 nsp16–nsp10 complex or hGNMT X = CH ₂ , Y = S, R = CH ₂ -C ₆ H ₃ -3-CO ₂ H,5-Ph: IC ₅₀ 0.58 ± 0.03 nM; nsp14 X = CH ₂ Y = S, R = CH ₂ -C ₆ H ₃ -3-CO ₂ H: IC ₅₀ 4 ± 0.5 nM; nsp16/nsp10	[103,104]
7.14/D ^d	<p>X = S(O)₂, C(O) R¹ = substituted phenyl R² = H, Et, alkyl (39 compounds)</p>	Inhibition of SARS-CoV-2 nsp14 X = S(O) ₂ , R ¹ = C ₆ H ₃ -3-CN,4-OMe, R ² = Et: IC ₅₀ 0.019 μM	[105]
7.15/D	<p>R = NO₂, NH₂, CF₃, Me, Cl, NHAc n = 1 or 2 (20 compounds)</p>	Inhibition of SARS-CoV-2 nsp14 R = 4-NO ₂ , n = 1: 40% inhibition of SARS-CoV-2 nsp14 at the compound concentration of 5 μM	[106]
7.16/D ^d	<p>R² = H, Ac, isobutyryl R³ = H or Ac X = CH₂, C(O), S(O)₂ Y = N or CH Z = C or N R¹ = naphth-2-yl, quinolin-7-yl, 2-Cl-quinolin-6-yl (11 compounds)</p>	Inhibition of SARS-CoV-2 nsp14 X = S(O) ₂ , Y = CH, Z = N, R ¹ = naphth-2-yl, R ² = H, R ³ = H: IC ₅₀ 0.093 μM; nsp14 EC ₅₀ 0.72 μM; SARS-CoV-2; A459 AT CC ₅₀ > 100 μM; A459 AT	[107]

Table 7. Cont.

Entry ^a /DRD Approach, Structure and Number of Compounds Examined	Object of Study ^b Antiviral Effect(s) If Given ^c	Ref.	
7.17/D ^d	<p data-bbox="316 607 810 683">R¹ = Br, Me, OMe; R² = Cl, NO₂, CN; R³ = H, Me, Et; X = OH or NHMe; Y = Ph or quinolin-3-yl (26 compounds)</p>	<p data-bbox="855 421 1225 622">Inhibition of SARS-CoV nsp14, SARS-CoV-2 nsp14, MERS-CoV nsp14 R¹ = OMe, R² = CN, R³ = Me, Y = quinolin-3-yl: IC₅₀ 0.141 ± 0.02 nM; SARS-CoV nsp14 IC₅₀ 0.72 ± 0.4 nM; SARS-CoV-2 nsp14 R¹ = OMe, R² = CN, R³ = Me, Y = Ph: IC₅₀ 1.25 ± 0.25 nM; MERS-CoV nsp14</p>	[108]

Approach A: repurposing of known NAs, including approved drugs or their prodrugs. Approach D: development of de novo-designed NAs. ^a Entry numbers include the number of the table and the position of a compound (or a group of compounds) on the timeline, taking into account the year of publication of the references discussed. ^b Exemplified as the inhibitory compound concentration (IC₅₀) or in a descriptive form. ^c Effective compound concentration (EC₅₀), inhibitory compound concentration (IC₅₀), or cytotoxic compound concentration (CC₅₀). ^d See text for details.

Vedadi and coworkers screened a library of 161 in-house synthesized SAM-competitive MTase inhibitors and SAM analogs [94]. Among the identified screening hits (entry 7.6), compound SS148 inhibited nsp14 MTase activity (IC₅₀ value of 70 ± 6 nM) and was selective against 20 human protein lysine MTases. Interestingly, compound DS0464, with an IC₅₀ value of 1.1 ± 0.2 μM, showed a competitive pattern of inhibition with regard to both RNA and SAM. The docking studies suggested that DS0464 could act as a bifunctional inhibitor, occupying the cofactor site and extending into the substrate binding site of the enzyme. Moreover, compounds SS148 and WZ16 (entry 7.6)—analogs of sinefungin—are potent inhibitors of the methyltransferase nsp10–nsp16 complex [95]. The crystal structures of the SARS-CoV-2 nsp10–nsp16 2'-O-RNA methyltransferase binding compound SS148 or WZ16 revealed the binding of both compounds to the SAM/SAH binding pocket of nsp16 through interactions similar to those identified for SAM/SAH. A biochemical study indicated an SAM-competitive pattern of inhibition for both SS148 and WZ16. On the other hand, with regard to RNA, SS148 showed an apparent noncompetitive pattern of inhibition, whereas WZ16 featured an uncompetitive one. The latter suggested that RNA could bind first, and its binding increased the affinity of WZ16 for binding to the nsp10–nsp16 complex. Interestingly, SS148 and WZ16 inhibited the MTase activities of all seven HCoV-229E [96]. The docking studies with the inhibitors SS148 and WZ16 and the nsp16 proteins of these seven HCoVs revealed that the proteins were highly conserved and the mechanisms of their interaction with the SS148 and WZ16 inhibitors were nearly identical.

Kuzikov et al. performed a repurposing screening of compound libraries (ca. 8700 compounds) containing approved drugs, drug candidates, and small molecules considered safe in humans [97]. Apart from previously reported inhibitors of SARS-CoV-2 3CL-Pro, they found 62 compounds with IC₅₀ values < 1 μM. Among them, thioguanosine (entry 7.7) showed a dose-dependent effect on SARS-CoV-2 3CL-Pro and demonstrated a moderate anticytopathic effect in *Vero E6* cells but did not show a reduction in the virus RNA in *Vero E6* cells. The docking of thioguanosine into the main catalytic cavity of 3CL-Pro revealed that the main ligand–protein interactions might involve the most probable tautomer for thioguanosine with a thiol group rather than a thio-ketonic group.

Plemper and coworkers identified 4'-fluorouridine (entry 7.8) as an oral drug candidate to treat COVID-19 [98]. SARS-CoV-2 is sensitive to 4'-fluorouridine, with EC₅₀ values ranging from 0.2 to 0.6 μM against isolates from different donors. Studies on the mode of action of 4'-fluorouridine showed the incorporation of its triphosphate (4'-FIU-TP) into the SARS-CoV-2 RNA by the virus RdRp instead of uridine triphosphate. The multiple

incorporations of 4'-FIU-TP caused delayed polymerase stalling. 4'-fluorouridine was orally efficient against SARS-CoV-2 in a ferret model [98].

Zhao et al. reported the screening of 134 compounds from the Selleckchemicals NAs library using a cell-based SARS-CoV-2 RdRp assay [99]. As a result, four potent inhibitors of SARS-CoV-2 RdRp, including 5-iodotubercidin, were identified. Notably, the four compounds also displayed a dose-dependent inhibitory effect against both the HCoV-OC43 and HCoV-NL63 viruses in *HCT-8* or *LLC-MK2* cells. Further studies for the most potent compound, namely 5-iodotubercidin, showed that its activity is related to the inhibition of adenosine kinase.

Menachery and coworkers explored whether SARS-CoV-2 nsp16 activity could be targeted for therapeutic treatment [100]. Testing the effect of sinefungin on wild-type (WT) SARS-CoV-2 replication (entry 7.10), they observed a dose-dependent decrease in virus replication in *Vero E6* cells or *Calu3 2B4* cells. Moreover, the combination of sinefungin with a constant dose of IFN-I pretreatment drove the further attenuation of WT SARS-CoV-2 in *Vero E6* cells. However, a dose-dependent effect of sinefungin on the viability of *Vero E6* cells was noted. The authors suggested that these results indicated dose limitations in using sinefungin as a therapeutic treatment.

Ahmed-Belkacem et al. developed a broad group of adenine dinucleosides with the O-2' → C-5' connection via a variety of aminoethyl linkers (entry 7.11) [101]. Among them, the most active SARS-CoV nsp14 inhibitor showed submicromolar activity and was as potent as, but particularly more specific, than sinefungin. Molecular docking suggested that the inhibitor was bound to a pocket formed by the SAM and cap RNA binding sites of the examined enzyme.

Otava et al. performed detailed studies on 7-deaza-7-substituted analogs of SAH as potential inhibitors of SARS-CoV nsp14 (entry 7.12) [102]. These compounds exhibited high inhibitory activity (IC_{50} 3 ± 0.5 – 37 ± 7 nM). The most active inhibitor showed an SAM-competitive but RNA-noncompetitive pattern of inhibition. The molecular modeling and docking studies with the homology model SARS-CoV nsp14 in complex with nsp10 revealed that (a) a lipophilic substituent caused a significant increase in the activity of the examined compounds; (b) derivatives with a methylene bridge were significantly less active than those with a lipophilic substituent linked via the ethynyl group or the ethylene one; and (c) derivatives bearing bicyclic lipophilic substituents have comparable activity to each other [102].

Bobileva and coworkers obtained a broad panel of SAH analogs with a variety of surrogates of the homocysteine moiety and assayed them against SARS-CoV-2 nsp14 or the SARS-CoV-2 nsp16–nsp10 complex (entry 7.13) [103,104]. The derivative with the 3-(mercaptomethyl)benzoic acid moiety as the parent compound showed one-digit nanomolar inhibitory activity towards both of the examined enzymes. Structural modifications of the parent compound, notably variations in the location of the carboxylic group and/or the additional phenyl substituent within the benzoic acid skeleton, provided an inhibitor of SARS-CoV-2 nsp14, exhibiting a very high activity of IC_{50} 0.58 ± 0.03 nM and slightly improved cell permeability compared with the parent compound. Docking results suggested that this 3-phenylbenzoic acid derivative was a nsp14 bisubstrate inhibitor occupying both SAM and mRNA-binding sites.

Ahmed-Belkacem et al. identified several highly active inhibitors of SARS-CoV-2 nsp14 among a variety of 5'-deoxy-5'-sulfonamido/amido derivatives of adenosine (entry 7.14) [105]. The docking studies with the most active inhibitor supported the hypothesis of a bisubstrate mechanism of its action. The detected orientation of this inhibitor in the enzyme binding sites suggested that the 3-cyano-4-methoxybenzenesulfonamide ring clearly occupied the capguanosine binding pocket.

Bisubstrate inhibitors of SARS-CoV-2 nsp14 were developed by Jung et al. (entry 7.16) [107]. Using a biochemical assay employing an LC-MS/MS technique, they established that highly active inhibitors could be obtained by connecting an adenosine moiety with an aromatic ring through a sulfonamide group. This study resulted in the identification

of four compounds with IC_{50} values in the nanomolar range. Docking studies showed significant differences in the binding mode of naphthalene-containing derivatives varying in the nucleobase scaffold. Briefly, the same location of the nucleobase (adenine or its 5-aza-7-deaza counterpart) resulted in substantially different interactions between protein residues and the sugar side moiety. These *in silico* observations supported the *in vitro* results. More importantly, one of the compounds, a 2-naphthyl derivative, also displayed high antiviral activity against SARS-CoV-2 in A549 cells and low cytotoxicity in the host cells, resulting in $SI > 139$. Interestingly, sinefungin, used as a reference compound, did not show antiviral activity in A549 cells [107].

Debart and coworkers, using a structure-guided drug design approach based on bisubstrate inhibitors, developed a number of compounds acting as adenosine mimetics with a variously substituted arylsulfonamide substituent at the 5'-position (entry 7.17) [108]. The adenine moiety was replaced with hypoxanthine, N^6 -methyladenine, or C^7 -substituted 7-deazaadenine. In this way, a highly selective inhibitor of SARS-CoV-2 nsp14 and SARS-CoV nsp14 with subnanomolar IC_{50} values was discovered ($R^1 = OMe$, $R^2 = CN$, $R^3 = Me$, $Y = \text{quinolin-3-yl}$). Docking analyses with this inhibitor suggested that C^7 -substituted 7-deazaadenine superimposed perfectly with the adenine of the SAM in the nsp14 structures, while the 3-quinoline or the phenyl substituent on the nucleobase protruded into the SAM entry channel. Moreover, an inhibitor of MERS-CoV nsp14 was also found ($R^1 = OMe$, $R^2 = CN$, $R^3 = Me$, $Y = Ph$). Further *in vitro* studies (*Vero E6 TMPRSS2* cells) on the most active compounds revealed that the C^7 -quinolin-ethynyl-substituted compounds showed moderate activities, reaching 50% SARS-CoV-2 (B.1) inhibition at 10 μM . Compounds with a phenyl-ethynyl substituent at the C^7 -position of the adenine moiety did not display any inhibitory activity. These results were interpreted in terms of delivery or stability problems [108].

2. Conclusions

Our literature survey revealed that over four hundred NAs (including prodrugs) were evaluated against HCoVs. Approach A (i.e., the repurposing of compounds existing in the public domain) appeared as the most often applied. It led to the identification of several active compounds. Some of them were approved as anti-COVID-19 drugs (e.g., remdesivir and molnupiravir). Bemnifosbuvir (entry 2.12) received an FDA fast-track status [18]. The high activities of bemnifosbuvir against SARS-CoV-1 (entry 1.32), MERS-CoV (entry 3.9), HCoV-OC43 (entry 4.11), and HCoV-229E (entry 5.7) made this compound a very attractive drug candidate for future medication for other and emerging HCoVs.

The repurposing strategy also exposed several NAs of interest, i.e., compounds with submicromolar *in vitro* activity: 6-azauridine (entry 1.1), pyrazofurin (entry 1.2), 2'-deoxytubercidin (entry 1.6), tubercidin (entries 2.10, 4.12, and 5.8), 5-hydroxymethyltubercidin (entries 2.14, 4.13, and 5.9), thioguanosine (entry 2.18), gemcitabine (entry 2.19), 6-thioinosine (entry 2.20), 3-deazaneplanocin A (entry 2.21), sangivamycin (entry 2.22), riboprime (entry 2.25), forodesine (entry 2.26), and 7-(furan-2-yl)tubercidin (entry 2.31). Some of these compounds suffered from low SI values (e.g., 2'-deoxytubercidin, entry 1.6) or specific limitations, e.g., serious side effects within a specific group of patients (6-azauridine [109]), or nephrotoxicity (in rodents, 3-deazaneplanocin A [110]; or in humans, tubercidin [111]). However, the reported anti-HCoV activities of these NAs might serve as starting points in the development of their further structural modifications.

The screening of large libraries of available compounds was used to search for antiviral agents—entry 1.28 (290 approved drugs with antiviral activities against other RNA viruses); entries 2.10, 2.14, 2.15, and 2.16 (753 nucleoside analogs from a compound library of Hokkaido University); and entries 2.10, 2.18, 2.19, and 2.20 (approximately 18,000 drugs, most of which have been tested in humans)—as well as for inhibitors of specific viral enzymes—entry 7.6 (161 in-house synthesized S-adenosylmethionine (SAM)-competitive MTase inhibitors and SAM analogs), entry 7.7 (8702 drugs and drug candidates from the repurposing collections), and entry 7.9 (134 compounds in the Selleckchemicals NAs library).

This fast way to identify prospective drugs seemed reasonable in an emergency case, such as COVID-19, where no proven therapeutic solution existed. However, considering the overall number of NAs collected in this review, we may conclude that the library screening revealed a relatively narrow group of compounds with promising properties.

The aristeromycin fluoro-analogs, with their submicromolar *in vitro* activities against SARS-CoV-1 and MERS-CoV (entries 1.38 and 3.10, respectively) and activity against SARS-CoV-2 (entry 2.39), underlined the case of the development of *de novo*-designed NAs (approach D), even if their SI values were still unfavorable. On the other hand, the *de novo*-designed sulfonamide inhibitors of SARS-CoV-2 nsp14 (entry 7.16) showed both submicromolar activity against SARS-CoV-2 and low cytotoxicity *in vitro*.

The prodrug concept was successfully implemented in the very recently released anti-COVID-19 drug candidates (bemnifosbuvir, Figure 1; and obeldesivir, entry 2.34). Furthermore, novel lipid prodrugs of GS-441524 (entries 2.33 and 5.12) were reported. Their significantly higher or comparable *in vitro* activities to those of remdesivir or GS-441524, satisfactory SI values, and convenient chemical synthesis made these compounds interesting targets.

NAs offer a large number of ways for the prodrug concept to be applied: (a) introducing a progroup into the glycone (entries 2.33, 5.12, and 2.34) or the nucleobase (entry 2.35); (b) employing a proven-in-practice progroup (such as phosphoramidate or isobutyryl, Figure 1, entries 1.38, 3.10, 2.34) or an investigational one (entries 2.4, 4.3, 2.31, 2.33, 5.12, 2.35, 2.40, 5.14); and (c) the involvement of all the reactive functional groups in the parent nucleoside scaffold (Figure 1, VV116; or entries 2.4, 4.3, 2.35, 2.40, 5.14) or just the selected one (Figure 1, entries 2.4, 4.3, 2.31, 2.33, 5.12, 2.34). Owing to the high reactivity of their functional groups, in particular in combination with the prodrug concept, NAs offered the formation of multi-element sets of derivatives (entries 2.31, 7.13, 7.14, 7.15, 7.16, 7.17). This approach has been extensively applied since 2021.

NAs were valuable tools for recognizing HCoV-related enzymes as potential drug targets. NAs inhibiting HCoV-related enzymes *in vitro* at submicromolar or subnanomolar concentrations were reported: SARS-CoV nsp14 (entries 7.1, 7.6, 7.11, 7.12, 7.17); SARS-CoV-2 nsp14 (entries 7.6, 7.13, 7.14, 7.16, 7.17); SARS-CoV-2 RdRp (entry 7.9); the SARS-CoV-2 nsp16 complex (entry 7.10); and the HCoV-NL63 nsp10–nsp16 complex (entry 7.6). Compounds with inhibitory activity towards methyltransferases of a broad panel of HCoVs were also identified (entry 7.6). In most cases, these nucleoside inhibitors were inactive against human methyltransferases (entries 7.6, 7.11, 7.12, and 7.17).

Among inhibitors of the HCoV-related enzymes, compounds endowed with antiviral activity against HCoVs *in vitro* were identified: anti-SARS-CoV-2 activity (entries 7.7, 7.10, and 7.16), anti-HCoV-OC43, or anti-HCoV-NL63 activity (entry 7.9). Moreover, compounds with anti-SARS-CoV-2 activity in an animal model were found (entry 7.8).

Currently, interventional clinical trials on three NAs have been completed: remdesivir [112–122], molnupiravir [123–126], and AT-527 [127]. The results of these studies were posted at ClinicalTrials.gov.

Recently, a hypothesis on the involvement of more than one virus in long COVID has been postulated [128]. The reactivation of viruses that had infected the patient previously was suggested. Clinical studies conducted by the biotechnology company Virios Therapeutics showed that a combination of valacyclovir and celecoxib, designed to synergistically suppress herpes virus replication, caused clinically and statistically significant improvements in fatigue, pain, and symptoms of autonomic dysfunction and general well-being related to long COVID in patients [129]. These findings might open up new horizons for the exploration of NAs as drugs in the treatment of SARS-CoV-2-related ailments.

Author Contributions: Both authors contributed equally to this manuscript. All authors have read and agreed to the published version of the manuscript.

Funding: This work was financially supported by the Warsaw University of Technology. Grant Number 504/04114/1020/44.000000.

Data Availability Statement: No new data were created or analyzed in this study. Data sharing is not applicable to this article.

Conflicts of Interest: The authors declare no conflicts of interest.

Abbreviations

3CL-Pro	3C-like protease
A459 cells	adenocarcinomic human alveolar basal epithelial cells
ATP	adenosine triphosphate
BHK-21 cells	baby hamster kidney fibroblast cells
Calu-3 cells	human lung cells
Caco-2 cells	human colorectal adenocarcinoma cells
CC ₅₀	50% cytotoxic concentration
DBT-9 cells	delayed brain tumor, murine astrocytoma clone 9
DMTr	dimethoxytrityl
EC ₅₀	50% effective concentration
fRhK4 cells	fetal rhesus monkey kidney cells
H460 cells	human nonsmall cell lung cancer cells
HAE cells	human tracheobronchial epithelial cells
HCT-8 cells	human ileocecal adenocarcinoma cells
HEK 293T cells	human embryonic kidney cells
HEL cells	human embryonic lung cells
Huh7 cells	well differentiated hepatocyte-derived carcinoma cells
HSV-1	herpes simplex virus 1
HSV-2	herpes simplex virus 2
IC ₅₀	50% cytotoxic concentration
IFN-I	Interferon type I
K _D	protein–ligand dissociation constant
LLC-MK2 cells	rhesus monkey kidney epithelial cells
MCC cells	Merkel cell carcinoma
MRC-5 cells	human fetal lung fibroblast cells
nsp14	RNA cap guanine-N7-methyltransferase
nsp16–nsp10	2'-O-methyltransferase nsp16–nsp10 complex
RD cells	rhabdomyosarcoma cells
RdRp	RNA-dependent RNA polymerase
SAH	S-adenosyl-L-homocysteine
SAM	S-adenosyl-L-methionine
SCC-VII	squamous cell carcinoma
TBDMS	tert-butyldimethylsilyl
TC ₅₀	50% toxic concentration
TP	–[P(O)(OH)O] ₃ H
Vero cells	Green Monkey kidney epithelial cells
Vero 118 cells	Vero cells clone 118
Vero 76 cells	Vero cells clone 76
Vero E6 cells	Vero cells clone E6
Vero E6 TMPRSS2 cells	human transmembrane serine protease 2-expressing Vero E6 cells

References

1. Weiss, S.R. Forty Years with Coronaviruses. *J. Exp. Med.* **2020**, *217*, e20200537. [[CrossRef](#)]
2. Guarner, J. Three Emerging Coronaviruses in Two Decades. *Am. J. Clin. Pathol.* **2020**, *153*, 420–421. [[CrossRef](#)]
3. WHO Regional Office for the Western Pacific. *SARS: How a Global Epidemic Was Stopped*; WHO Regional Office for the Western Pacific: Manila, Philippines, 2006; ISBN 978-92-9061-213-1.
4. Azhar, E.I.; Hui, D.S.C.; Memish, Z.A.; Drosten, C.; Zumla, A. The Middle East Respiratory Syndrome (MERS). *Infect. Dis. Clin. N. Am.* **2019**, *33*, 891–905. [[CrossRef](#)]
5. Middle East Respiratory Syndrome Coronavirus (MERS-CoV). Available online: <https://www.who.int/health-topics/middle-east-respiratory-syndrome-coronavirus-mers> (accessed on 5 June 2023).

6. Weekly Epidemiological Update on COVID-19—1 June 2023. Available online: <https://www.who.int/publications/m/item/weekly-epidemiological-update-on-covid-19---1-june-2023> (accessed on 5 June 2023).
7. WHO Chief Declares End to COVID-19 as a Global Health Emergency | UN News. Available online: <https://news.un.org/en/story/2023/05/1136367> (accessed on 5 June 2023).
8. Marra, M.A.; Jones, S.J.M.; Astell, C.R.; Holt, R.A.; Brooks-Wilson, A.; Butterfield, Y.S.N.; Khattra, J.; Asano, J.K.; Barber, S.A.; Chan, S.Y.; et al. The Genome Sequence of the SARS-Associated Coronavirus. *Science* **2003**, *300*, 1399–1404. [[CrossRef](#)]
9. Kandeil, A.; Shehata, M.M.; El Shesheny, R.; Gomaa, M.R.; Ali, M.A.; Kayali, G. Complete Genome Sequence of Middle East Respiratory Syndrome Coronavirus Isolated from a Dromedary Camel in Egypt. *Genome Announc.* **2016**, *4*, e00309-16. [[CrossRef](#)]
10. Naqvi, A.A.T.; Fatima, K.; Mohammad, T.; Fatima, U.; Singh, I.K.; Singh, A.; Atif, S.M.; Hariprasad, G.; Hasan, G.M.; Hassan, M.d.I. Insights into SARS-CoV-2 Genome, Structure, Evolution, Pathogenesis and Therapies: Structural Genomics Approach. *Biochim. Biophys. Acta BBA Mol. Basis Dis.* **2020**, *1866*, 165878. [[CrossRef](#)]
11. Morse, J.S.; Lalonde, T.; Xu, S.; Liu, W.R. Learning from the Past: Possible Urgent Prevention and Treatment Options for Severe Acute Respiratory Infections Caused by 2019-nCoV. *ChemBioChem* **2020**, *21*, 730–738. [[CrossRef](#)]
12. Li, G.; De Clercq, E. Therapeutic Options for the 2019 Novel Coronavirus (2019-nCoV). *Nat. Rev. Drug Discov.* **2020**, *19*, 149–150. [[CrossRef](#)]
13. Martinez, M.A. Compounds with Therapeutic Potential against Novel Respiratory 2019 Coronavirus. *Antimicrob. Agents Chemother.* **2020**, *64*, e00399-20. [[CrossRef](#)]
14. Pastuch-Gawolek, G.; Gillner, D.; Król, E.; Walczak, K.; Wandzik, I. Selected Nucleos(t)ide-Based Prescribed Drugs and Their Multi-Target Activity. *Eur. J. Pharmacol.* **2019**, *865*, 172747. [[CrossRef](#)]
15. Koren, G.; King, S.; Knowles, S.; Phillips, E. Ribavirin in the Treatment of SARS: A New Trick for an Old Drug? *CMAJ Can. Med. Assoc. J.* **2003**, *168*, 1289–1292.
16. Barnard, D.L.; Day, C.W.; Bailey, K.; Heiner, M.; Montgomery, R.; Lauridsen, L.; Winslow, S.; Hoopes, J.; Li, J.K.-K.; Lee, J.; et al. Enhancement of the Infectivity of SARS-CoV in BALB/c Mice by IMP Dehydrogenase Inhibitors, Including Ribavirin. *Antivir. Res.* **2006**, *71*, 53–63. [[CrossRef](#)]
17. Li, G.; Hilgenfeld, R.; Whitley, R.; De Clercq, E. Therapeutic Strategies for COVID-19: Progress and Lessons Learned. *Nat. Rev. Drug Discov.* **2023**, *22*, 449–475. [[CrossRef](#)]
18. Horga, A.; Kuritzkes, D.R.; Kowalczyk, J.J.; Pietropaolo, K.; Belanger, B.; Lin, K.; Perkins, K.; Hammond, J. Phase II Study of Bemnifosbuvir in High-Risk Participants in a Hospital Setting with Moderate COVID-19. *Future Virol.* **2023**, *18*, 489–500. [[CrossRef](#)]
19. Jordan, P.C.; Stevens, S.K.; Deval, J. Nucleosides for the Treatment of Respiratory RNA Virus Infections. *Antivir. Chem. Chemother.* **2018**, *26*, 1–19. [[CrossRef](#)]
20. Pruijssers, A.J.; Denison, M.R. Nucleoside Analogues for the Treatment of Coronavirus Infections. *Curr. Opin. Virol.* **2019**, *35*, 57–62. [[CrossRef](#)]
21. Totura, A.L.; Bavari, S. Broad-Spectrum Coronavirus Antiviral Drug Discovery. *Expert Opin. Drug Discov.* **2019**, *14*, 397–412. [[CrossRef](#)]
22. Yan, J.; Liu, A.; Huang, J.; Wu, J.; Fan, H. Research Progress of Drug Treatment in Novel Coronavirus Pneumonia. *AAPS PharmSciTech* **2020**, *21*, 130. [[CrossRef](#)]
23. Ami, E.; Ohru, H. Intriguing Antiviral Modified Nucleosides: A Retrospective View into the Future Treatment of COVID-19. *ACS Med. Chem. Lett.* **2021**, *12*, 510–517. [[CrossRef](#)]
24. Roy, V.; Agrofoglio, L.A. Nucleosides and Emerging Viruses: A New Story. *Drug Discov. Today* **2022**, *27*, 1945–1953. [[CrossRef](#)]
25. Borbone, N.; Piccialli, G.; Roviello, G.N.; Oliviero, G. Nucleoside Analogs and Nucleoside Precursors as Drugs in the Fight against SARS-CoV-2 and Other Coronaviruses. *Molecules* **2021**, *26*, 986. [[CrossRef](#)]
26. Thames, J.E.; Seley-Radtke, K.L. Comparison of the Old and New—Novel Mechanisms of Action for Anti-Coronavirus Nucleoside Analogues. *CHIMIA* **2022**, *76*, 409–417. [[CrossRef](#)]
27. Xu, X.; Chen, Y.; Lu, X.; Zhang, W.; Fang, W.; Yuan, L.; Wang, X. An Update on Inhibitors Targeting RNA-Dependent RNA Polymerase for COVID-19 Treatment: Promises and Challenges. *Biochem. Pharmacol.* **2022**, *205*, 115279. [[CrossRef](#)]
28. Bekheit, M.S.; Panda, S.S.; Girgis, A.S. Potential RNA-Dependent RNA Polymerase (RdRp) Inhibitors as Prospective Drug Candidates for SARS-CoV-2. *Eur. J. Med. Chem.* **2023**, *252*, 115292. [[CrossRef](#)]
29. Zenchenko, A.A.; Drenichev, M.S.; Mikhailov, S.N. Nucleoside Inhibitors of Coronaviruses. *Curr. Med. Chem.* **2021**, *28*, 5284–5310. [[CrossRef](#)]
30. Cinatl, J.; Morgenstern, B.; Bauer, G.; Chandra, P.; Rabenau, H.; Doerr, H.W. Glycyrrhizin, an Active Component of Licorice Roots, and Replication of SARS-Associated Coronavirus. *Lancet* **2003**, *361*, 2045–2046. [[CrossRef](#)]
31. Barnard, D.L.; Hubbard, V.D.; Burton, J.; Smee, D.F.; Morrey, J.D.; Otto, M.J.; Sidwell, R.W. Inhibition of Severe Acute Respiratory Syndrome-Associated Coronavirus (SARSCoV) by Calpain Inhibitors and Beta-D-N4-Hydroxycytidine. *Antivir. Chem. Chemother.* **2004**, *15*, 15–22. [[CrossRef](#)]
32. Barnard, D.L.; Day, C.W.; Bailey, K.; Heiner, M.; Montgomery, R.; Lauridsen, L.; Chan, P.K.; Sidwell, R.W. Evaluation of Immunomodulators, Interferons and Known in Vitro SARS-CoV Inhibitors for Inhibition of SARS-Cov Replication in BALB/c Mice. *Antivir. Chem. Chemother.* **2006**, *17*, 275–284. [[CrossRef](#)]

33. Günther, S.; Asper, M.; Röser, C.; Luna, L.K.S.; Drosten, C.; Becker-Ziaja, B.; Borowski, P.; Chen, H.-M.; Hosmane, R.S. Application of Real-Time PCR for Testing Antiviral Compounds against Lassa Virus, SARS Coronavirus and Ebola Virus in Vitro. *Antivir. Res.* **2004**, *63*, 209–215. [CrossRef]
34. Chen, F.; Chan, K.H.; Jiang, Y.; Kao, R.Y.T.; Lu, H.T.; Fan, K.W.; Cheng, V.C.C.; Tsui, W.H.W.; Hung, I.F.N.; Lee, T.S.W.; et al. In Vitro Susceptibility of 10 Clinical Isolates of SARS Coronavirus to Selected Antiviral Compounds. *J. Clin. Virol.* **2004**, *31*, 69–75. [CrossRef]
35. Saijo, M.; Morikawa, S.; Fukushi, S.; Mizutani, T.; Hasegawa, H.; Nagata, N.; Iwata, N.; Kurane, I. Inhibitory Effect of Mizoribine and Ribavirin on the Replication of Severe Acute Respiratory Syndrome (SARS)-Associated Coronavirus. *Antivir. Res.* **2005**, *66*, 159–163. [CrossRef]
36. Sheahan, T.P.; Sims, A.C.; Zhou, S.; Graham, R.L.; Pruijssers, A.J.; Agostini, M.L.; Leist, S.R.; Schäfer, A.; Dinno, K.H.; Stevens, L.J.; et al. An Orally Bioavailable Broad-Spectrum Antiviral Inhibits SARS-CoV-2 in Human Airway Epithelial Cell Cultures and Multiple Coronaviruses in Mice. *Sci. Transl. Med.* **2020**, *12*, eabb5883. [CrossRef]
37. Ikejiri, M.; Saijo, M.; Morikawa, S.; Fukushi, S.; Mizutani, T.; Kurane, I.; Maruyama, T. Synthesis and Biological Evaluation of Nucleoside Analogues Having 6-Chloropurine as Anti-SARS-CoV Agents. *Bioorganic Med. Chem. Lett.* **2007**, *17*, 2470–2473. [CrossRef]
38. Chu, C.K.; Gadthula, S.; Chen, X.; Choo, H.; Olgen, S.; Barnard, D.L.; Sidwell, R.W. Antiviral Activity of Nucleoside Analogues against SARS-Coronavirus (SARS-CoV). *Antivir. Chem. Chemother.* **2006**, *17*, 285–289. [CrossRef]
39. Dyal, J.; Coleman, C.M.; Hart, B.J.; Venkataraman, T.; Holbrook, M.R.; Kindrachuk, J.; Johnson, R.F.; Olinger, G.G.; Jahrling, P.B.; Laidlaw, M.; et al. Repurposing of Clinically Developed Drugs for Treatment of Middle East Respiratory Syndrome Coronavirus Infection. *Antimicrob. Agents Chemother.* **2014**, *58*, 4885–4893. [CrossRef]
40. Warren, T.K.; Wells, J.; Panchal, R.G.; Stuthman, K.S.; Garza, N.L.; Van Tongeren, S.A.; Dong, L.; Retterer, C.J.; Eaton, B.P.; Pegoraro, G.; et al. Protection against Filovirus Diseases by a Novel Broad-Spectrum Nucleoside Analogue BCX4430. *Nature* **2014**, *508*, 402–405. [CrossRef]
41. Peters, H.L.; Jochmans, D.; de Wilde, A.H.; Posthuma, C.C.; Snijder, E.J.; Neyts, J.; Seley-Radtke, K.L. Design, Synthesis and Evaluation of a Series of Acyclic Fleximer Nucleoside Analogues with Anti-Coronavirus Activity. *Bioorganic Med. Chem. Lett.* **2015**, *25*, 2923–2926. [CrossRef]
42. Sheahan, T.P.; Sims, A.C.; Graham, R.L.; Menachery, V.D.; Gralinski, L.E.; Case, J.B.; Leist, S.R.; Pyrc, K.; Feng, J.Y.; Trantcheva, I.; et al. Broad-Spectrum Antiviral GS-5734 Inhibits Both Epidemic and Zoonotic Coronaviruses. *Sci. Transl. Med.* **2017**, *9*, eaal3653. [CrossRef]
43. Agostini, M.L.; Andres, E.L.; Sims, A.C.; Graham, R.L.; Sheahan, T.P.; Lu, X.; Smith, E.C.; Case, J.B.; Feng, J.Y.; Jordan, R.; et al. Coronavirus Susceptibility to the Antiviral Remdesivir (GS-5734) Is Mediated by the Viral Polymerase and the Proofreading Exoribonuclease. *mBio* **2018**, *9*, e00221-18. [CrossRef]
44. Good, S.S.; Westover, J.; Jung, K.H.; Zhou, X.-J.; Moussa, A.; La Colla, P.; Collu, G.; Canard, B.; Sommadossi, J.-P. AT-527, a Double Prodrug of a Guanosine Nucleotide Analog, Is a Potent Inhibitor of SARS-CoV-2 In Vitro and a Promising Oral Antiviral for Treatment of COVID-19. *Antimicrob. Agents Chemother.* **2021**, *65*, aac.02479-20. [CrossRef]
45. Cho, J.H.; Bernard, D.L.; Sidwell, R.W.; Kern, E.R.; Chu, C.K. Synthesis of Cyclopentenyl Carbocyclic Nucleosides as Potential Antiviral Agents Against Orthopoxviruses and SARS. *J. Med. Chem.* **2006**, *49*, 1140–1148. [CrossRef]
46. Cho, A.; Saunders, O.L.; Butler, T.; Zhang, L.; Xu, J.; Vela, J.E.; Feng, J.Y.; Ray, A.S.; Kim, C.U. Synthesis and Antiviral Activity of a Series of 1'-Substituted 4-Aza-7,9-Dideazaadenosine C-Nucleosides. *Bioorganic Med. Chem. Lett.* **2012**, *22*, 2705–2707. [CrossRef]
47. Yoon, J.; Kim, G.; Jarhad, D.B.; Kim, H.-R.; Shin, Y.-S.; Qu, S.; Sahu, P.K.; Kim, H.O.; Lee, H.W.; Wang, S.B.; et al. Design, Synthesis, and Anti-RNA Virus Activity of 6'-Fluorinated-Aristeromycin Analogues. *J. Med. Chem.* **2019**, *62*, 6346–6362. [CrossRef]
48. ClinicalTrials.gov [Internet]. U.S. National Library of Medicine. Identifier NCT03891420. A Study to Evaluate the Safety, Pharmacokinetics and Antiviral Effects of Galidesivir in Yellow Fever or COVID-19. 2019. Available online: <https://classic.clinicaltrials.gov/ct2/show/NCT03891420?term=NCT03891420&draw=2&rank=1> (accessed on 22 April 2024).
49. BioCryst. Provides Update on Galidesivir Program | BioCryst Pharmaceuticals. Available online: <https://ir.biocryst.com/news-releases/news-release-details/biocryst-provides-update-galidesivir-program> (accessed on 19 June 2023).
50. Taylor, R.; Bowen, R.; Demarest, J.F.; DeSpirito, M.; Hartwig, A.; Bielefeldt-Ohmann, H.; Walling, D.M.; Mathis, A.; Babu, Y.S. Activity of Galidesivir in a Hamster Model of SARS-CoV-2. *Viruses* **2021**, *14*, 8. [CrossRef]
51. Ogando, N.S.; Zevenhoven-Dobbe, J.C.; Jarhad, D.B.; Tripathi, S.K.; Lee, H.W.; Jeong, L.S.; Snijder, E.J.; Posthuma, C.C. 6',6'-Difluoro-Aristeromycin Is a Potent Inhibitor of MERS-Coronavirus Replication. *bioRxiv* **2021**. [CrossRef]
52. Zandi, K.; Amblard, F.; Musall, K.; Downs-Bowen, J.; Kleinbard, R.; Oo, A.; Cao, D.; Liang, B.; Russell, O.O.; McBrayer, T.; et al. Repurposing Nucleoside Analogs for Human Coronaviruses. *Antimicrob. Agents Chemother.* **2020**, *65*, e01652-20. [CrossRef]
53. Xie, Y.; Yin, W.; Zhang, Y.; Shang, W.; Wang, Z.; Luan, X.; Tian, G.; Aisa, H.A.; Xu, Y.; Xiao, G.; et al. Design and Development of an Oral Remdesivir Derivative VV116 against SARS-CoV-2. *Cell Res.* **2021**, *31*, 1212–1214. [CrossRef]
54. Schultz, D.C.; Johnson, R.M.; Ayyanathan, K.; Miller, J.; Whig, K.; Kamalia, B.; Dittmar, M.; Weston, S.; Hammond, H.L.; Dillen, C.; et al. Pyrimidine Inhibitors Synergize with Nucleoside Analogues to Block SARS-CoV-2. *Nature* **2022**, *604*, 134–140. [CrossRef]
55. Wang, M.; Cao, R.; Zhang, L.; Yang, X.; Liu, J.; Xu, M.; Shi, Z.; Hu, Z.; Zhong, W.; Xiao, G. Remdesivir and Chloroquine Effectively Inhibit the Recently Emerged Novel Coronavirus (2019-nCoV) in Vitro. *Cell Res.* **2020**, *30*, 269–271. [CrossRef]

56. Uemura, K.; Nobori, H.; Sato, A.; Sanaki, T.; Toba, S.; Sasaki, M.; Murai, A.; Saito-Tarashima, N.; Minakawa, N.; Orba, Y.; et al. 5-Hydroxymethyltubercidin Exhibits Potent Antiviral Activity against Flaviviruses and Coronaviruses, Including SARS-CoV-2. *iScience* **2021**, *24*, 103120. [CrossRef]
57. Sacramento, C.Q.; Fintelman-Rodrigues, N.; Temerozo, J.R.; Da Silva, A.d.P.D.; Dias, S.d.S.G.; da Silva, C.d.S.; Ferreira, A.C.; Mattos, M.; Pão, C.R.R.; de Freitas, C.S.; et al. In Vitro Antiviral Activity of the Anti-HCV Drugs Daclatasvir and Sofosbuvir against SARS-CoV-2, the Aetiological Agent of COVID-19. *J. Antimicrob. Chemother.* **2021**, *76*, 1874–1885. [CrossRef] [PubMed]
58. Ellinger, B.; Bojkova, D.; Zaliani, A.; Cinatl, J.; Claussen, C.; Westhaus, S.; Keminer, O.; Reinshagen, J.; Kuzikov, M.; Wolf, M.; et al. A SARS-CoV-2 Cytotoxicity Dataset Generated by High-Content Screening of a Large Drug Repurposing Collection. *Sci. Data* **2021**, *8*, 70. [CrossRef] [PubMed]
59. Bergant, V.; Yamada, S.; Grass, V.; Tsukamoto, Y.; Lavacca, T.; Krey, K.; Mühlhofer, M.-T.; Wittmann, S.; Ensser, A.; Herrmann, A.; et al. Attenuation of SARS-CoV-2 Replication and Associated Inflammation by Concomitant Targeting of Viral and Host Cap 2'-O-Ribose Methyltransferases. *EMBO J.* **2022**, *41*, e111608. [CrossRef] [PubMed]
60. Bennett, R.P.; Postnikova, E.N.; Eaton, B.P.; Cai, Y.; Yu, S.; Smith, C.O.; Liang, J.; Zhou, H.; Kocher, G.A.; Murphy, M.J.; et al. Sangivamycin Is Highly Effective against SARS-CoV-2 in Vitro and Has Favorable Drug Properties. *JCI Insight* **2022**, *7*, e153165. [CrossRef] [PubMed]
61. Rabie, A.M. Potent Inhibitory Activities of the Adenosine Analogue Cordycepin on SARS-CoV-2 Replication. *ACS Omega* **2022**, *7*, 2960–2969. [CrossRef] [PubMed]
62. Rabie, A.M. Efficacious Preclinical Repurposing of the Nucleoside Analogue Didanosine against COVID-19 Polymerase and Exonuclease. *ACS Omega* **2022**, *7*, 21385–21396. [CrossRef] [PubMed]
63. Rabie, A.M.; Abdalla, M. A Series of Adenosine Analogs as the First Efficacious Anti-SARS-CoV-2 Drugs against the B.1.1.529.4 Lineage: A Preclinical Repurposing Research Study. *ChemistrySelect* **2022**, *7*, e202201912. [CrossRef] [PubMed]
64. Abdalla, M.; Rabie, A.M. Dual Computational and Biological Assessment of Some Promising Nucleoside Analogs against the COVID-19-Omicron Variant. *Comput. Biol. Chem.* **2023**, *104*, 107768. [CrossRef] [PubMed]
65. Rabie, A.M.; Abdalla, M. Forodesine and Riboprime Exhibit Strong Anti-SARS-CoV-2 Repurposing Potential: In Silico and In Vitro Studies. *ACS Bio Med Chem Au* **2022**, *2*, 565–585. [CrossRef] [PubMed]
66. Rabie, A.M.; Abdalla, M. Evaluation of a Series of Nucleoside Analogs as Effective Anticoronaviral-2 Drugs against the Omicron-B.1.1.529/BA.2 Subvariant: A Repurposing Research Study. *Med. Chem. Res.* **2023**, *32*, 326–341. [CrossRef] [PubMed]
67. Lin, X.; Ke, X.; Jian, X.; Xia, L.; Yang, Y.; Zhang, T.; Xiong, H.; Zhao, B.; Liu, W.; Chen, Q.; et al. Azacytidine Targeting SARS-CoV-2 Viral RNA as a Potential Treatment for COVID-19. *Sci. Bull.* **2022**, *67*, 1022–1025. [CrossRef] [PubMed]
68. Yu, B.; Chang, J. Azvudine (FNC): A Promising Clinical Candidate for COVID-19 Treatment. *Signal Transduct. Target. Ther.* **2020**, *5*, 236. [CrossRef] [PubMed]
69. Zhang, J.-L.; Li, Y.-H.; Wang, L.-L.; Liu, H.-Q.; Lu, S.-Y.; Liu, Y.; Li, K.; Liu, B.; Li, S.-Y.; Shao, F.-M.; et al. Azvudine Is a Thymus-Homing Anti-SARS-CoV-2 Drug Effective in Treating COVID-19 Patients. *Signal Transduct. Target. Ther.* **2021**, *6*, 414. [CrossRef] [PubMed]
70. Yu, B.; Chang, J. The First Chinese Oral Anti-COVID-19 Drug Azvudine Launched. *Innov. Camb. Mass* **2022**, *3*, 100321. [CrossRef] [PubMed]
71. Milisavljevic, N.; Konkolová, E.; Kozák, J.; Hodek, J.; Veselovská, L.; Sýkorová, V.; Čížek, K.; Pohl, R.; Eyer, L.; Svoboda, P.; et al. Antiviral Activity of 7-Substituted 7-Deazapurine Ribonucleosides, Monophosphate Prodrugs, and Triphosphates against Emerging RNA Viruses. *ACS Infect. Dis.* **2021**, *7*, 471–478. [CrossRef] [PubMed]
72. Schooley, R.T.; Carlin, A.F.; Beadle, J.R.; Valiaeva, N.; Zhang, X.-Q.; Clark, A.E.; McMillan, R.E.; Leibel, S.L.; McVicar, R.N.; Xie, J.; et al. Rethinking Remdesivir: Synthesis, Antiviral Activity, and Pharmacokinetics of Oral Lipid Prodrugs. *Antimicrob. Agents Chemother.* **2021**, *65*, aac.01155-21. [CrossRef] [PubMed]
73. Lo, M.K.; Shrivastava-Ranjan, P.; Chatterjee, P.; Flint, M.; Beadle, J.R.; Valiaeva, N.; Murphy, J.; Schooley, R.T.; Hostetler, K.Y.; Montgomery, J.M.; et al. Broad-Spectrum In Vitro Antiviral Activity of ODBG-P-RVn: An Orally-Available, Lipid-Modified Monophosphate Prodrug of Remdesivir Parent Nucleoside (GS-441524). *Microbiol. Spectr.* **2021**, *9*, e01537-21. [CrossRef] [PubMed]
74. Cao, L.; Li, Y.; Yang, S.; Li, G.; Zhou, Q.; Sun, J.; Xu, T.; Yang, Y.; Liao, R.; Shi, Y.; et al. The Adenosine Analog Prodrug ATV006 Is Orally Bioavailable and Has Preclinical Efficacy against Parental SARS-CoV-2 and Variants. *Sci. Transl. Med.* **2022**, *14*, eabm7621. [CrossRef] [PubMed]
75. Wen, Z.-H.; Wang, M.-M.; Li, L.-Y.; Herdewijn, P.; Snoeck, R.; Andrei, G.; Liu, Z.-P.; Liu, C. Synthesis and Anti-SARS-CoV-2 Evaluation of Lipid Prodrugs of β -D-N4-Hydroxycytidine (NHC) and a 3'-Fluoro-Substituted Analogue of NHC. *Bioorganic Chem.* **2023**, *135*, 106527. [CrossRef] [PubMed]
76. Bege, M.; Kiss, A.; Bereczki, I.; Hodek, J.; Polyák, L.; Szemán-Nagy, G.; Naesens, L.; Weber, J.; Borbás, A. Synthesis and Anticancer and Antiviral Activities of C-2'-Branched Arabinonucleosides. *Int. J. Mol. Sci.* **2022**, *23*, 12566. [CrossRef] [PubMed]
77. Tonix Seeks to Advance OyaGen's COVID-19 Treatment Under New Global Licensing Deal. Available online: <https://www.biospace.com/article/tonix-seeks-to-advance-oyagen-s-covid-19-treatment-under-new-global-licensing-deal/> (accessed on 24 September 2023).
78. Bibi, S.; Hasan, M.M.; Wang, Y.-B.; Papadakos, S.P.; Yu, H. Cordycepin as a Promising Inhibitor of SARS-CoV-2 RNA Dependent RNA Polymerase (RdRp). *Curr. Med. Chem.* **2022**, *29*, 152–162. [CrossRef] [PubMed]

79. Ye, Y. China Approves First Homegrown COVID Antiviral. In *Nature*; Springer Nature Limited: London, UK, 26 July 2022. [[CrossRef](#)]
80. McCarthy, M.W. VV116 as a Potential Treatment for COVID-19. *Expert Opin. Pharmacother.* **2023**, *24*, 675–678. [[CrossRef](#)] [[PubMed](#)]
81. Chan, J.F.W.; Chan, K.-H.; Kao, R.Y.T.; To, K.K.W.; Zheng, B.-J.; Li, C.P.Y.; Li, P.T.W.; Dai, J.; Mok, F.K.Y.; Chen, H.; et al. Broad-Spectrum Antivirals for the Emerging Middle East Respiratory Syndrome Coronavirus. *J. Infect.* **2013**, *67*, 606–616. [[CrossRef](#)] [[PubMed](#)]
82. Warren, T.K.; Jordan, R.; Lo, M.K.; Ray, A.S.; Mackman, R.L.; Soloveva, V.; Siegel, D.; Perron, M.; Bannister, R.; Hui, H.C.; et al. Therapeutic Efficacy of the Small Molecule GS-5734 against Ebola Virus in Rhesus Monkeys. *Nature* **2016**, *531*, 381–385. [[CrossRef](#)] [[PubMed](#)]
83. Agostini, M.L.; Pruijssers, A.J.; Chappell, J.D.; Gribble, J.; Lu, X.; Andres, E.L.; Bluemling, G.R.; Lockwood, M.A.; Sheahan, T.P.; Sims, A.C.; et al. Small-Molecule Antiviral β -d-N4-Hydroxycytidine Inhibits a Proofreading-Intact Coronavirus with a High Genetic Barrier to Resistance. *J. Virol.* **2019**, *93*, e01348-19. [[CrossRef](#)] [[PubMed](#)]
84. Parang, K.; El-Sayed, N.S.; Kazeminy, A.J.; Tiwari, R.K. Comparative Antiviral Activity of Remdesivir and Anti-HIV Nucleoside Analogues against Human Coronavirus 229E (HCoV-229E). *Molecules* **2020**, *25*, 2343. [[CrossRef](#)] [[PubMed](#)]
85. Głowacka, I.E.; Andrei, G.; Schols, D.; Snoeck, R.; Gawron, K. Design, Synthesis, and the Biological Evaluation of a New Series of Acyclic 1,2,3-Triazole Nucleosides. *Arch. Pharm.* **2017**, *350*, e1700166. [[CrossRef](#)] [[PubMed](#)]
86. Pyrc, K.; Bosch, B.J.; Berkhout, B.; Jebbink, M.F.; Dijkman, R.; Rottier, P.; Hoek, L. van der Inhibition of Human Coronavirus NL63 Infection at Early Stages of the Replication Cycle. *Antimicrob. Agents Chemother.* **2006**, *50*, 2000–2008. [[CrossRef](#)] [[PubMed](#)]
87. Bouvet, M.; Debarnot, C.; Imbert, I.; Selisko, B.; Snijder, E.J.; Canard, B.; Decroly, E. In Vitro Reconstitution of SARS-Coronavirus mRNA Cap Methylation. *PLoS Pathog.* **2010**, *6*, e1000863, Correction in *PLoS Pathog.* **2010**, *6*. [[CrossRef](#)]
88. Aouadi, W.; Blanjoie, A.; Vasseur, J.-J.; Debart, F.; Canard, B.; Decroly, E. Binding of the Methyl Donor S-Adenosyl-L-Methionine to Middle East Respiratory Syndrome Coronavirus 2'-O-Methyltransferase Nsp16 Promotes Recruitment of the Allosteric Activator Nsp10. *J. Virol.* **2016**, *91*, e02217-16. [[CrossRef](#)] [[PubMed](#)]
89. Gordon, C.J.; Tchesnokov, E.P.; Woolner, E.; Perry, J.K.; Feng, J.Y.; Porter, D.P.; Götte, M. Remdesivir Is a Direct-Acting Antiviral That Inhibits RNA-Dependent RNA Polymerase from Severe Acute Respiratory Syndrome Coronavirus 2 with High Potency. *J. Biol. Chem.* **2020**, *295*, 6785–6797. [[CrossRef](#)] [[PubMed](#)]
90. Ju, J.; Li, X.; Kumar, S.; Jockusch, S.; Chien, M.; Tao, C.; Morozova, I.; Kalachikov, S.; Kirchdoerfer, R.N.; Russo, J.J. Nucleotide Analogues as Inhibitors of SARS-CoV Polymerase. *Pharmacol. Res. Perspect.* **2020**, *8*, e00674. [[CrossRef](#)] [[PubMed](#)]
91. Chien, M.; Anderson, T.K.; Jockusch, S.; Tao, C.; Li, X.; Kumar, S.; Russo, J.J.; Kirchdoerfer, R.N.; Ju, J. Nucleotide Analogues as Inhibitors of SARS-CoV-2 Polymerase, a Key Drug Target for COVID-19. *J. Proteome Res.* **2020**, *19*, 4690–4697. [[CrossRef](#)] [[PubMed](#)]
92. Jockusch, S.; Tao, C.; Li, X.; Chien, M.; Kumar, S.; Morozova, I.; Kalachikov, S.; Russo, J.J.; Ju, J. Sofosbuvir Terminated RNA Is More Resistant to SARS-CoV-2 Proofreader than RNA Terminated by Remdesivir. *Sci. Rep.* **2020**, *10*, 16577. [[CrossRef](#)] [[PubMed](#)]
93. Lu, G.; Zhang, X.; Zheng, W.; Sun, J.; Hua, L.; Xu, L.; Chu, X.; Ding, S.; Xiong, W. Development of a Simple In Vitro Assay To Identify and Evaluate Nucleotide Analogs against SARS-CoV-2 RNA-Dependent RNA Polymerase. *Antimicrob. Agents Chemother.* **2020**, *65*, e01508-20. [[CrossRef](#)] [[PubMed](#)]
94. Devkota, K.; Schapira, M.; Perveen, S.; Khalili Yazdi, A.; Li, F.; Chau, I.; Ghiabi, P.; Hajian, T.; Loppnau, P.; Bolotokova, A.; et al. Probing the SAM Binding Site of SARS-CoV-2 Nsp14 In Vitro Using SAM Competitive Inhibitors Guides Developing Selective Bisubstrate Inhibitors. *SLAS Discov. Adv. Life Sci. R D* **2021**, *26*, 1200–1211. [[CrossRef](#)] [[PubMed](#)]
95. Klima, M.; Khalili Yazdi, A.; Li, F.; Chau, I.; Hajian, T.; Bolotokova, A.; Kaniskan, H.Ü.; Han, Y.; Wang, K.; Li, D.; et al. Crystal Structure of SARS-CoV-2 Nsp10–Nsp16 in Complex with Small Molecule Inhibitors, SS148 and WZ16. *Protein Sci.* **2022**, *31*, e4395. [[CrossRef](#)] [[PubMed](#)]
96. Li, F.; Ghiabi, P.; Hajian, T.; Klima, M.; Li, A.S.M.; Khalili Yazdi, A.; Chau, I.; Loppnau, P.; Kutera, M.; Seitova, A.; et al. SS148 and WZ16 Inhibit the Activities of Nsp10–Nsp16 Complexes from All Seven Human Pathogenic Coronaviruses. *Biochim. Biophys. Acta Gen. Subj.* **2023**, *1867*, 130319. [[CrossRef](#)] [[PubMed](#)]
97. Kuzikov, M.; Costanzi, E.; Reinshagen, J.; Esposito, F.; Vangeel, L.; Wolf, M.; Ellinger, B.; Claussen, C.; Geisslinger, G.; Corona, A.; et al. Identification of Inhibitors of SARS-CoV-2 3CL-Pro Enzymatic Activity Using a Small Molecule in Vitro Repurposing Screen. *ACS Pharmacol. Transl. Sci.* **2021**, *4*, 1096–1110. [[CrossRef](#)] [[PubMed](#)]
98. Sourimant, J.; Lieber, C.M.; Aggarwal, M.; Cox, R.M.; Wolf, J.D.; Yoon, J.-J.; Toots, M.; Ye, C.; Sticher, Z.; Kolykhalov, A.A.; et al. 4'-Fluorouridine Is an Oral Antiviral That Blocks Respiratory Syncytial Virus and SARS-CoV-2 Replication. *Science* **2022**, *375*, 161–167. [[CrossRef](#)] [[PubMed](#)]
99. Zhao, J.; Liu, Q.; Yi, D.; Li, Q.; Guo, S.; Ma, L.; Zhang, Y.; Dong, D.; Guo, F.; Liu, Z.; et al. 5-Iodobutercidin Inhibits SARS-CoV-2 RNA Synthesis. *Antivir. Res.* **2022**, *198*, 105254. [[CrossRef](#)] [[PubMed](#)]
100. Schindewolf, C.; Lokugamage, K.; Vu, M.N.; Johnson, B.A.; Scharton, D.; Plante, J.A.; Kalveram, B.; Crocquet-Valdes, P.A.; Sotcheff, S.; Jaworski, E.; et al. SARS-CoV-2 Uses Nonstructural Protein 16 To Evade Restriction by IFIT1 and IFIT3. *J. Virol.* **2023**, *97*, e01532-22. [[CrossRef](#)] [[PubMed](#)]
101. Ahmed-Belkacem, R.; Sutto-Ortiz, P.; Guiraud, M.; Canard, B.; Vasseur, J.-J.; Decroly, E.; Debart, F. Synthesis of Adenine Dinucleosides SAM Analogues as Specific Inhibitors of SARS-CoV Nsp14 RNA Cap Guanine-N7-Methyltransferase. *Eur. J. Med. Chem.* **2020**, *201*, 112557. [[CrossRef](#)] [[PubMed](#)]

102. Otava, T.; Šála, M.; Li, F.; Fanfrlík, J.; Devkota, K.; Perveen, S.; Chau, I.; Pakarian, P.; Hobza, P.; Vedadi, M.; et al. The Structure-Based Design of SARS-CoV-2 Nsp14 Methyltransferase Ligands Yields Nanomolar Inhibitors. *ACS Infect. Dis.* **2021**, *7*, 2214–2220. [[CrossRef](#)] [[PubMed](#)]
103. Bobileva, O.; Bobrovs, R.; Kaņepe, I.; Patetko, L.; Kalniņš, G.; Šišovs, M.; Bula, A.L.; Gri Nberga, S.; Boroduškis, M.R.; Ramata-Stunda, A.; et al. Potent SARS-CoV-2 mRNA Cap Methyltransferase Inhibitors by Bioisosteric Replacement of Methionine in SAM Cosubstrate. *ACS Med. Chem. Lett.* **2021**, *12*, 1102–1107. [[CrossRef](#)]
104. Bobileva, O.; Bobrovs, R.; Sirma, E.E.; Kanepe, I.; Bula, A.L.; Patetko, L.; Ramata-Stunda, A.; Grinberga, S.; Jirgensons, A.; Jaudzems, K. 3-(Adenosylthio)Benzoic Acid Derivatives as SARS-CoV-2 Nsp14 Methyltransferase Inhibitors. *Molecules* **2023**, *28*, 768. [[CrossRef](#)] [[PubMed](#)]
105. Ahmed-Belkacem, R.; Hausdorff, M.; Delpal, A.; Sutto-Ortiz, P.; Colmant, A.M.G.; Touret, F.; Ogando, N.S.; Snijder, E.J.; Canard, B.; Coutard, B.; et al. Potent Inhibition of SARS-CoV-2 Nsp14 N7-Methyltransferase by Sulfonamide-Based Bisubstrate Analogues. *J. Med. Chem.* **2022**, *65*, 6231–6249. [[CrossRef](#)] [[PubMed](#)]
106. Amador, R.; Delpal, A.; Canard, B.; Vasseur, J.-J.; Decroly, E.; Debart, F.; Clavé, G.; Smietana, M. Facile Access to 4'-(N-Acylsulfonamide) Modified Nucleosides and Evaluation of Their Inhibitory Activity against SARS-CoV-2 RNA Cap N7-Guanine-Methyltransferase Nsp14. *Org. Biomol. Chem.* **2022**, *20*, 7582–7586. [[CrossRef](#)] [[PubMed](#)]
107. Jung, E.; Soto-Acosta, R.; Xie, J.; Wilson, D.J.; Dreis, C.D.; Majima, R.; Edwards, T.C.; Geraghty, R.J.; Chen, L. Bisubstrate Inhibitors of Severe Acute Respiratory Syndrome Coronavirus-2 Nsp14 Methyltransferase. *ACS Med. Chem. Lett.* **2022**, *13*, 1477–1484. [[CrossRef](#)] [[PubMed](#)]
108. Hausdorff, M.; Delpal, A.; Barelier, S.; Nicollet, L.; Canard, B.; Touret, F.; Colmant, A.; Coutard, B.; Vasseur, J.-J.; Decroly, E.; et al. Structure-Guided Optimization of Adenosine Mimetics as Selective and Potent Inhibitors of Coronavirus Nsp14 N7-Methyltransferases. *Eur. J. Med. Chem.* **2023**, *256*, 115474. [[CrossRef](#)] [[PubMed](#)]
109. Elis, J.; Rašková, H. New Indications for 6-Azauridine Treatment in Man. A Review. *Eur. J. Clin. Pharmacol.* **1972**, *4*, 77–81. [[CrossRef](#)] [[PubMed](#)]
110. Sun, F.; Lee, L.; Zhang, Z.; Wang, X.; Yu, Q.; Duan, X.; Chan, E. Preclinical Pharmacokinetic Studies of 3-Deazaneplanocin A, a Potent Epigenetic Anticancer Agent, and Its Human Pharmacokinetic Prediction Using GastroPlusTM. *Eur. J. Pharm. Sci.* **2015**, *77*, 290–302. [[CrossRef](#)] [[PubMed](#)]
111. Bisel, H.F.; Ansfield, F.; Mason, J.H.; Wilson, W. Clinical Studies with Tubercidin Administered by Direct Intravenous Injection. *Cancer Res.* **1970**, *30*, 76–78. [[PubMed](#)]
112. ClinicalTrials.gov [Internet]. U.S. National Library of Medicine. Identifier NCT04280705. Adaptive COVID-19 Treatment Trial (ACTT). 2020. Available online: <https://classic.clinicaltrials.gov/ct2/show/NCT04280705?term=NCT04280705&draw=2&rank=1> (accessed on 22 April 2024).
113. ClinicalTrials.gov [Internet]. U.S. National Library of Medicine. Identifier NCT04292730. Study to Evaluate the Safety and Antiviral Activity of Remdesivir (GS-5734TM) in Participants with Moderate Coronavirus Disease (COVID-19) Compared to Standard of Care Treatment. 2020. Available online: <https://classic.clinicaltrials.gov/ct2/show/NCT04292730?term=NCT04292730&draw=2&rank=1> (accessed on 22 April 2024).
114. ClinicalTrials.gov [Internet]. U.S. National Library of Medicine. Identifier NCT04292899. Study to Evaluate the Safety and Antiviral Activity of Remdesivir (GS-5734TM) in Participants with Severe Coronavirus Disease (COVID-19). 2020. Available online: <https://classic.clinicaltrials.gov/ct2/show/NCT04292899?term=NCT04292899&draw=2&rank=1> (accessed on 22 April 2024).
115. ClinicalTrials.gov [Internet]. U.S. National Library of Medicine. Identifier NCT04401579. Adaptive COVID-19 Treatment Trial 2 (ACTT-2). 2020. Available online: <https://classic.clinicaltrials.gov/ct2/show/NCT04401579?term=NCT04401579&draw=2&rank=1> (accessed on 22 April 2024).
116. ClinicalTrials.gov [Internet]. U.S. National Library of Medicine. Identifier NCT04409262. A Study to Evaluate the Efficacy and Safety of Remdesivir Plus Tocilizumab Compared with Remdesivir Plus Placebo in Hospitalized Participants with Severe COVID-19 Pneumonia (REMDACTA). 2020. Available online: <https://classic.clinicaltrials.gov/ct2/show/NCT04409262?term=NCT04409262&draw=2&rank=1> (accessed on 22 April 2024).
117. ClinicalTrials.gov [Internet]. U.S. National Library of Medicine. Identifier NCT04492475. Adaptive COVID-19 Treatment Trial 3 (ACTT-3). 2020. Available online: <https://classic.clinicaltrials.gov/ct2/show/NCT04492475?term=NCT04492475&draw=2&rank=1> (accessed on 22 April 2024).
118. ClinicalTrials.gov [Internet]. U.S. National Library of Medicine. Identifier NCT04539262. Study in Participants with Early Stage Coronavirus Disease 2019 (COVID-19) to Evaluate the Safety, Efficacy, and Pharmacokinetics of Remdesivir Administered by Inhalation. 2020. Available online: <https://classic.clinicaltrials.gov/ct2/show/NCT04539262?term=NCT04539262&draw=2&rank=1> (accessed on 22 April 2024).
119. ClinicalTrials.gov [Internet]. U.S. National Library of Medicine. Identifier NCT04546581. Inpatient Treatment of COVID-19 with Anti-Coronavirus Immunoglobulin (ITAC). 2020. Available online: <https://classic.clinicaltrials.gov/ct2/show/NCT04546581?term=NCT04546581&draw=2&rank=1> (accessed on 22 April 2024).
120. ClinicalTrials.gov [Internet]. U.S. National Library of Medicine. Identifier NCT04583956. ACTIV-5/Big Effect Trial (BET-A) for the Treatment of COVID-19. 2020. Available online: <https://classic.clinicaltrials.gov/ct2/show/NCT04583956?term=NCT04583956&draw=2&rank=1> (accessed on 22 April 2024).

121. ClinicalTrials.gov [Internet]. U.S. National Library of Medicine. Identifier NCT04593940. Immune Modulators for Treating COVID-19 (ACTIV-1 IM). 2020. Available online: <https://classic.clinicaltrials.gov/ct2/show/NCT04593940?term=NCT04593940&draw=2&rank=1> (accessed on 22 April 2024).
122. ClinicalTrials.gov [Internet]. U.S. National Library of Medicine. Identifier NCT04988035. ACTIV-5/Big Effect Trial (BET-C) for the Treatment of COVID-19. 2021. Available online: <https://classic.clinicaltrials.gov/ct2/show/NCT04988035?term=NCT04988035&draw=2&rank=1> (accessed on 22 April 2024).
123. ClinicalTrials.gov [Internet]. U.S. National Library of Medicine. Identifier NCT04405570. Safety, Tolerability and Efficacy of Molnupiravir (EIDD-2801) to Eliminate Infectious Virus Detection in Persons with COVID-19. 2020. Available online: <https://classic.clinicaltrials.gov/ct2/show/NCT04405570?term=NCT04405570&draw=2&rank=1> (accessed on 22 April 2024).
124. ClinicalTrials.gov [Internet]. U.S. National Library of Medicine. Identifier NCT04392219. COVID-19 First in Human Study to Evaluate Safety, Tolerability, and Pharmacokinetics of EIDD-2801 in Healthy Volunteers. 2020. Available online: <https://classic.clinicaltrials.gov/ct2/show/NCT04392219?term=NCT04392219&draw=2&rank=1> (accessed on 22 April 2024).
125. ClinicalTrials.gov [Internet]. U.S. National Library of Medicine. Identifier NCT04405739. The Safety of Molnupiravir (EIDD-2801) and Its Effect on Viral Shedding of SARS-CoV-2 (END-COVID). 2020. Available online: <https://classic.clinicaltrials.gov/ct2/show/NCT04405739?term=NCT04405739&draw=2&rank=1> (accessed on 22 April 2024).
126. ClinicalTrials.gov [Internet]. U.S. National Library of Medicine. Identifier NCT04575597. Efficacy and Safety of Molnupiravir (MK-4482) in Non-Hospitalized Adult Participants with COVID-19 (MK-4482-002). 2020. Available online: <https://classic.clinicaltrials.gov/ct2/show/NCT04575597?term=NCT04575597&draw=2&rank=1> (accessed on 22 April 2024).
127. ClinicalTrials.gov [Internet]. U.S. National Library of Medicine. Identifier NCT04709835. Study to Evaluate the Effects of AT-527 in Non-Hospitalized Adult Patients with Mild or Moderate COVID-19. 2021. Available online: <https://classic.clinicaltrials.gov/ct2/show/NCT04709835?term=NCT04709835&draw=2&rank=1> (accessed on 22 April 2024).
128. Kim, S.E. Long COVID: The Hunt for Causes and Cures. Available online: <https://cen.acs.org/biological-chemistry/infectious-disease/Long-COVID-hunt-causes-cures/101/i30> (accessed on 19 September 2023).
129. Virios Therapeutics Announces Positive Data Demonstrating Improvement in Multiple Long-COVID Symptoms Following Treatment with a Combination of Valacyclovir and Celecoxib in an Exploratory, Open-Label, Proof of Concept Study. Available online: <https://ir.virios.com/news/press-releases/detail/100/virios-therapeutics-announces-positive-data-demonstrating> (accessed on 18 September 2023).

Disclaimer/Publisher's Note: The statements, opinions and data contained in all publications are solely those of the individual author(s) and contributor(s) and not of MDPI and/or the editor(s). MDPI and/or the editor(s) disclaim responsibility for any injury to people or property resulting from any ideas, methods, instructions or products referred to in the content.